Commission of the European Communities

JOINT
RESEARCH
CENTRE

NEANDC (E) 292 "U" Vol. III Euratom

INDC (EUR) 022/G

XN8800146

ANNUAL PROGRESS REPORT ON NUCLEAR DATA 1987

CENTRAL BUREAU FOR NUCLEAR MEASUREMENTS

GEEL (BELGIUM)

October 1988

Commission of the European Communities

NEANDC (E) 292 "U" Vol. III Euratom

INDC (EUR) 022/G

JOINT
RESEARCH
CENTRE

ANNUAL PROGRESS REPORT ON NUCLEAR DATA 1987

CENTRAL BUREAU FOR NUCLEAR MEASUREMENTS

GEEL (BELGIUM)

October 1988

TABLE OF CONTENTS

EXECUTIVE SUMMARY

A.J. Deruytter

In the 1984-1987 multiannual research programme of CBNM, JRC-Geel, the project Nuclear Measurements is concerned with Nuclear Data and Nuclear Metrology.

In 1987 the efforts for the improvement of the set of standard neutron cross-sections and other quantities selected within the INDC/NEANDC Standard File continued. Widths of TKE- and mass-distributions in the fission of ^{235}U as a function of neutron energy and variation of these distributions as function of the resonances and their quantum numbers can be successfully described on the basis of a three exit channel fission model. The measurements on ^{252}Cf indicate that the overwhelming part of the fission neutrons are emitted from the fully accelerated fragments. A new measurement of the 59.5 keV gamma-ray emission probability in the ^{241}Am decay was published.

In the field of nuclear data for fission technology effort was concentrated on European requests in the NEA High Priority Request List. In the subthermal neutron energy region the measurements of η of ^{235}U previously reported were corrected for multiple scattering in a more complete manner, and first fission cross-section measurements were performed at the Very Cold Neutron Source of ILL Grenoble. The analysis of the data on the Cr isotopes has well progressed and measurements on Ni isotopes are underway. An experimental method for the determination of efficiencies and response functions of capture detectors, when applied to neutron capture measurements, is successful in reproducing the transmission results of the 1.15 keV resonance in ^{56}Fe, and resolves the discrepancy which initiated the NEANDC Task Force. It remains to be solved why the measured characteristics of these detectors are so different from predictions.

In the area of nuclear data for fusion technology, the measurements aim at an improvement of relevant data for neutron transport calculations in the blanket which contains lithium as tritium breeder material and for prediction of gas production. The method and the results of the experiment to determine double differential neutron emission cross-sections of ^{7}Li have been published. Also tritium production cross-sections for ^{9}Be in the energy range from threshold to 20 MeV were measured, in collaboration with KFA Jülich.

The radionuclide metrology follows three lines: determination of decay-scheme data, preparation of special standards and the improvement of measurement techniques including international comparisons. A method to improve the accuracy of peak analysis in high resolution alpha spectrometry has been published. An ionization chamber was calibrated and is operated on line for activity measurements. CBNM participated in an international trial comparison of activity-concentration measurements of a ^{125}I solution (BIPM).

In the field of metrology for neutron flux and dose CBNM participated in a comparison, organized by BIPM, to check the usefulness of the two spheres, technique at neutron energies of 2.5 and 14.7 MeV for neutron fluence determination. The CBNM Tissue Equivalent Plastic (TEP) calorimeter was commissioned. Absorbed-dose determinations by ionometric techniques were performed for neutron irradiations for the Radiobiology department of SCK/CEN Mol.

1 NUCLEAR DATA

1.1 NUCLEAR DATA FOR STANDARDS

In the area of nuclear data for standards the effort went mainly to neutron data and in particular to the ^{235}U fission cross-section standard and the standard fission neutron spectrum of ^{252}Cf, of which the results are described in some detail below. The evaluation of radionuclide decay data, in particular X- and γ-ray detector calibration data, in the framework of an IAEA coordinated research programme, was pursued. Emission probabilities of the 59.5 keV γ ray from ^{241}Am and of the α particles from ^{237}Np have been determined. Also the evaluation of X-ray emission probabilities is in progress.

1.1.1 Neutron Data for Standards

Fission Mode Fluctuations in Resonances of $^{235}U(n,f)$

H.-H. Knitter, F.-J. Hambsch,* C. Budtz-Jørgensen**, R. Vogt
(WRENDA request nr. 781192R)

Important for the use as a standard of the ^{235}U fission cross section are experimental data on the details of the mass-, energy-, and angular distributions of the fission fragments as function of neutron energy. In a previous experiment it was observed that the fragment average total kinetic energy at an incident neutron energy of only 500 keV is considerably higher than the thermal value. Also the fragment angular distributions showed a rather strong dependence on the incident neutron energy. To study the above-mentioned fission properties as function of neutron energy and in the resonance region as function of the resonances and their quantum numbers, an experiment at a 10 m flight-path station at the Geel electron linear accelerator (GELINA) was set up[1]. The measuring period for data taking ended in July 1986 and the evaluation of the large amount of experimental data was finished in 1987. The results of the present measurements are fission fragment yields, Y(M, TKE, cosδ, E_n), as a function of the fragment mass M, the total fragment kinetic energy TKE, the cosine of the angle δ between the incident neutron beam direction and the direction of propagation of the fission fragment, and the incident

---

* EC Fellow
** Danish Space Research Institute, DK-2800 Lyngby, Denmark
(1) Programme Progress Report, July-December 1985, COM. N° 4272

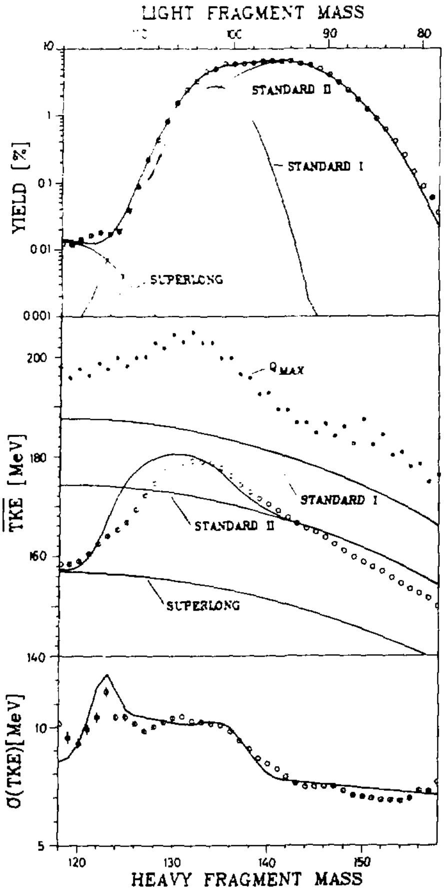

Fig. 1. The fission fragment yield from $^{235}U(n,f)$ at thermal energy, the average total kinetic energy, and sigma (TKE) are plotted versus the fragment mass.

neutron energy E_n. The measurements extend in incident neutron energy from thermal to 0.5 MeV. The angular dependence of the fragment emission is important at the higher incident neutron energy [2], whereas at low neutron energies, where only s-wave neutrons can participate in the fission reaction, the fragment emission probability is isotropic with respect to cosδ. The cosδ-dependence is not considered in the data evaluation for the resolved resonance region from thermal to about 140 eV, of which some of the results are presented.

The fragment yield for each isolated resonance or incident neutron energy bin Y(M, TKE) can be represented by the integrated mass distribution Y(M), the average total kinetic energy as function of mass split $\overline{TKE}(M)$, sigma (TKE) and higher moments of the TKE(M)-distributions.

Fig. 1 shows for the thermal neutron induced fission of $^{235}U(n,f)$ the experimental fission fragment mass distribution, the average total kinetic energy TKE as function of mass, and the square root of the variance of the TKE distribution as function of mass.

Recently, Brosa et al.[2] contributed to the interpretation of these distributions in terms of the fission process. They performed Strutinski-type calculations for several nuclei covering the mass range from ^{227}Ac to ^{258}Fm, where the potential energy of the compound system was calculated also for large deformations up to the scission point.

---

(1) Programme Progress Report, January-December 1986, COM. N° 4289

(2) U. Brosa, S. Grossmann, A. Müller, Z.Naturforschg. <u>41a</u>(1986)1341

These calculations indicate the presence of several fission modes, paths or exit channels, whose accessabilities are different for different fissioning nuclei. They predict the existence of three fission exit channels for $^{235}U(n,f)$, which result in three different scission shapes of the compound system. This picture of the fission process permits to develop a simple mathematical description for the fission fragment yield as function of fragment mass and total kinetic energy.

The total fission fragment mass distribution is a superposition of three Gaussian frequency distributions one for each fission exit channel. The mass distribution of each fission channel is determined by its relative population, and by the average mass and width of the Gaussian mass distribution. The three Gaussian distributions describing the superlong, standard I and standard II fission mode mass distributions are plotted in the upper part of Fig. 1 as full lines. The full line through the experimental points shows the sum of the three Gaussians. The curves were obtained by fitting the experimental mass distribution data for thermal neutron induced fission of ^{235}U. The values for the relative population W_i, average masses M_i and variances $\sigma^2(M_i)$ of the mass distributions for the three fission modes, are given in Table 1. In the above model a different but specific scission shape belongs to each fission mode which is characterized e.g. by the distance D_i between the two charge centres and their charge ratio. The total kinetic energy of the fragments is calculated as the Coulomb repulsion energy neglecting other smaller terms. The variance of the TKE distributions is obtained assuming a Gaussian frequency distribution for the charge distance D around the average D_i with a width $\sigma(D_i)$. This representation of the fission fragment yield as function of mass and TKE (see above reference) was used to fit the experimental data for the average total kinetic energy as function of mass $\overline{TKE}(M)$ and the square root of the variance of the TKE-distribution sigma (M). The parameters D_i and $\sigma(D_i)$ obtained by the fit are given in Table 1. In the middle part of Fig. 1 there are three thinner lines representing the $\overline{TKE}$ as function of mass for each fission exit channel. The thicker line, following the experimental points within 5 %, is the average total kinetic energy composed of those from the three exit channels. This model can explain also the drop of the TKE towards mass symmetry.

The most important parameters of the present description of the fission fragment yield as function of mass and TKE can also be obtained just by inspection of the fission fragment yield contour plot versus mass and TKE as shown in Fig. 2 for thermal neutron induced fission of $^{235}U(n,f)$. The average masses M_i and the average energies TKE_i for each channel are marked in Fig. 2 by dashed lines. This plot shows that the superlong fission path might have a small mass asymmetry of about 2 mass units. This correponds however to the resolution limit of the experiment.

Table 1. Comparison of parameters from experiment and theory

Channel name	Experiment					
	W_i [%]	M_i [u]	$\sigma^2(M_i)$ [u^2]	D_i [fm]	$\sigma(D_i)$ [fm]	TKE_i [MeV]
Superlong	0 069 ± 0 010	118	17 1 ± 6	19.4 ± 0 9	1 00 ± 0 68	157 ± 7
Standard I	18 3 ± 0 3	133 9 ± 0 1	6 9 ± 0.4	16 0 ± 0 1	0 69 ± 0 05	187 ± 1
Standard II	81 4 ± 0 4	141 1 ± 0 1	24 6 ± 0 4	17 5 ± 0 1	0 8 ± 0 01	167 ± 1
Channel name	Theory					
		M_i [u]	$\sigma^2(M_i)$ [u^2]	l_h/S' [fm]		TKE_i [MeV]
Superlong	----	118 ± 5	30 ± 15	19 2 ± 0 5	----	159 ± 4
Standard I	----	133 ± 5	4 3 ± 2 1	16 4 ± 0 5	---	183 ± 6
Standard II	----	147 ± 5	35 ± 17	19 0 ± 0.5	----	151 ± 4

The large σ values of the TKE distributions are not understood by any previous fission model[1]. As shown in the lower part of Fig. 1, the present description of a three exit channel model can cope also with the sigma distribution. Below mass 140 the superpositions of the exit channels are responsible for the higher values of $\sigma(TKE)$, since the exit channels have different average energies.
Mass and TKE distributions are evaluated for many isolated resonances of the compound nucleus ^{236}U and are analyzed and interpreted in the frame of the above, briefly described model.

---

[1] Oganessian and Lazarev, in Extreme Nuclear States, Vol. 4, D.A. Bromley (ed.), Plenum Press (New York-London)(1984), pp 1-255

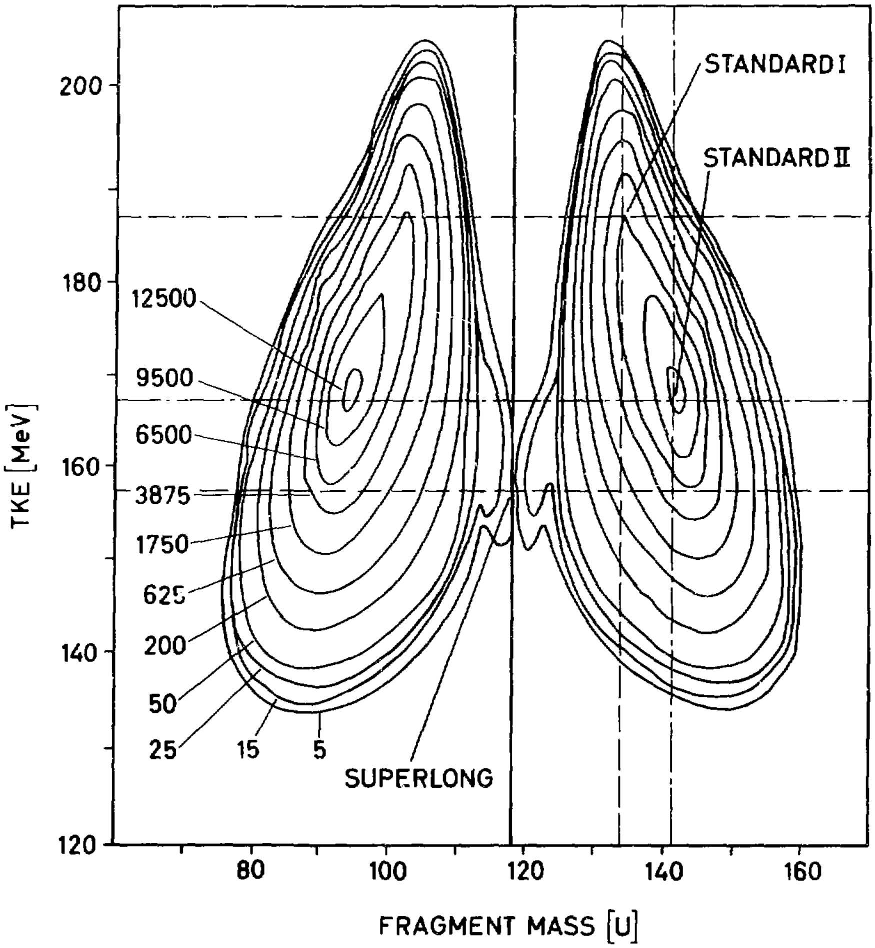

Fig. 2. Contour plot of fragment yield from $^{235}U(n,f)$

Fig. 3 shows in three parts, as an example for many resonances, the mass distribution for thermal neutron induced fission, and the difference and the ratio of the mass distribution measured for the 19.3 eV resonance with respect to the thermal distribution. The yield difference brings into evidence an increase of the population of the standard I channel and a decrease of the standard II channel with respect to the thermal distribution. The ratio of both spectra in the upper part of Fig. 2 shows a decrease of the symmetric fission yield by about a factor of two compared with the yield for thermal neutrons. The consequences of these experimental results for the understanding of the fission process are discussed in more detail in the above mentioned three publications.

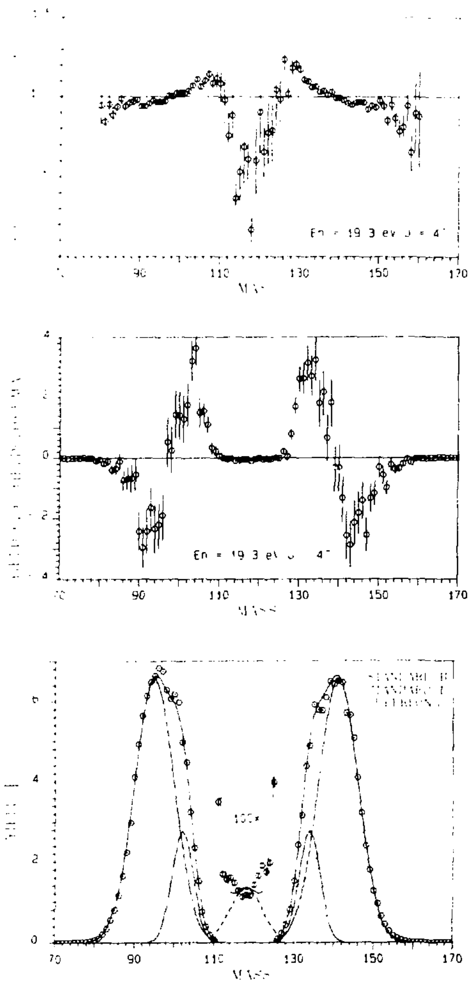

Fig. 3. The lower part shows the mass distribution of $^{235}U(n,f)$ for thermal neutrons, the full line through the experimental points is the sum of the mass distributions from the three exit chanels. The middle and upper parts show the experimental difference and the ratio of the mass distribution measured for the 19.3 eV, $J=4^-$ resonance with respect to the thermal distribution, respectively.

Investigation of Spontaneous Fission of ^{252}Cf

C. Budtz-Jørgensen*, H.-H. Knitter,
K. Vogt

(WRENDA request Nrs. 7?2189 R, 821026) The neutron energy spectrum of the spontaneous fission of ^{252}Cf is regarded as a neutron spectrum shape standard. This standard is widely used for neutron detector calibration purposes. It is however not clear with which mathematical parametrization the spectrum can be best described. Therefore more detailed experimental effort is needed to obtain a realistic, theory-based spectrum shape description. A multiparameter experiment for a detailed study of the prompt fission neutron spectrum was accomplished. The evaluation of the raw experimental data was continued and many of the results are now available in a final form and some of the results are presented. The neutron emission process in fission can have three origins:
(1) scission neutrons emitted from the compound system, (2) neutrons emitted from the fragments during their acceleration period, and (3) neutrons emitted from the fully accelerated fragments. All three processes have been considered in models, however without information about the partition between the three processes. The present correlation experiment between fission fragments and neutrons can give information on the partition of these processes to the total neutron emission in the spontaneous fission of ^{252}Cf. For this purpose, the neutron energies and

* Danish Space Research Institute, DK-2800 Lyngby, Denmark

emission angles with respect to the direction of propagation of the fragments were converted, event by event, to the centre of mass system of the fully accelerated fragments.

Fig. 4 shows the two dimensional spectrum of the yield versus the neutron energy in the fragment centre-of-mass system and versus the $\cos\delta_{CM}$ in the same reference system. This transformation yields isotropic angular distributions for all neutron energies within the experimental error.

This shows that the overwhelming part of the fission neutrons are emitted

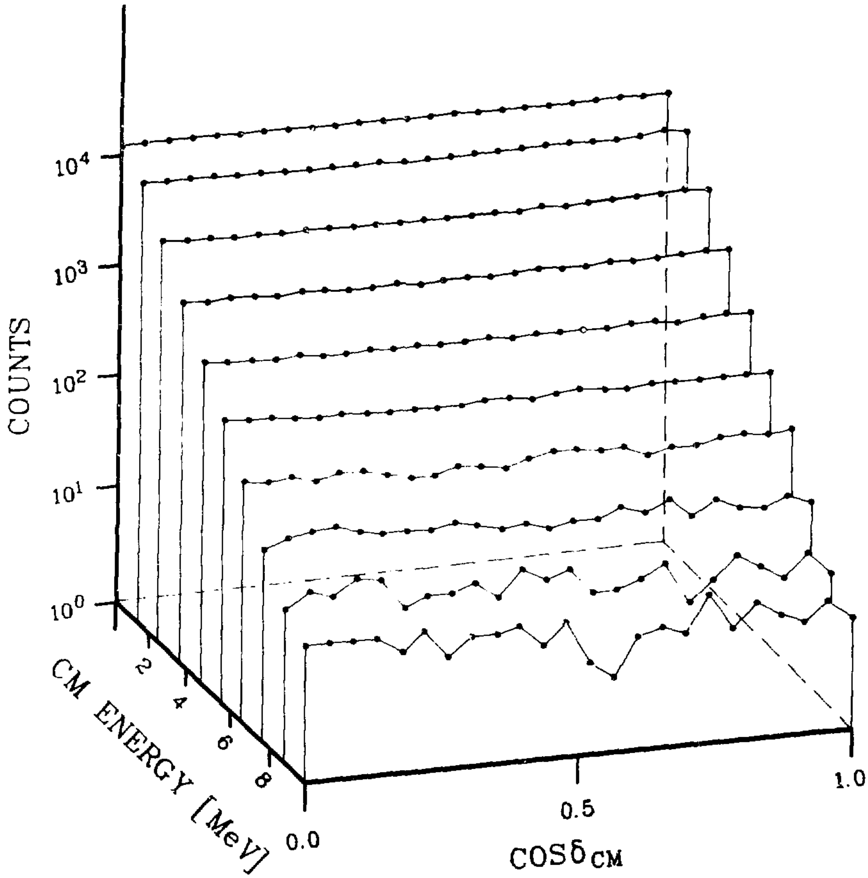

Fig. 4. Fission neutron yield versus the neutron energy in the fragment centre-of mass system and versus $\cos\delta_{CM}$

from the fully accelerated fragments. For a theoretical description of the standard fission neutron spectrum the level density parameter as function of fragment mass is needed. This important physical quantity can be obtained from the neutron spectra in the fragment centre-of-mass system which are available as function of fragment mass and fragment total kinetic energy.

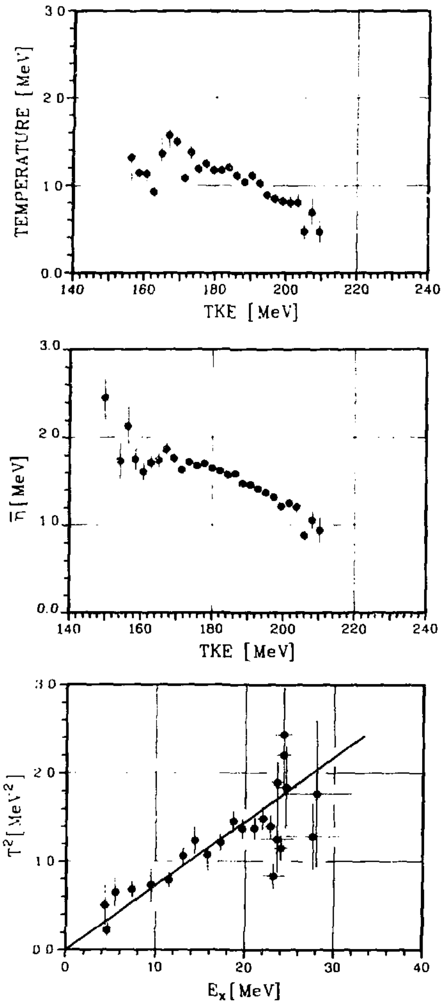

Fig. 5. In the middle and upper parts are plotted the nuclear temperature and the average neutron energy for the fragment mass 110 versus TKE, respectively. The lowest part shows T^2 versus the excitation energy. The straight line fits the experimental points.

Fig. 5 shows in the upper part for the fragment mass 110 the average neutron energy, $\bar{\eta}$ evaluated from those spectra, as function of the fragment kinetic energy TKE. In the middle part of Fig. 5 the nuclear temperature, evaluated from the neutron spectra, is given versus TKE also for fragment mass 110. The fragment excitation energy E_x can be obtained from the relation

$$E_x = \bar{\nu}(\mathrm{TKE})(B_n + \bar{\eta}(\mathrm{TKE}))$$

where B_n is the neutron binding energy and $\bar{\nu}(TKE)$ is the average number of neutrons emitted from the specific fragment at total kinetic energy TKE. $\bar{\nu}(TKE)$ is not shown but was also evaluated from the present measurements. The equation

$$E_x = a\,T^2$$

is valid between the excitation energy and the nuclear temperature in the frame of the Fermi-gas model, where a is the wanted level density parameter of the fission fragment. The lower part of Fig. 5 shows the experimental data of T^2 versus E_x. The slope of the straight line through the experimental points gives the level density parameter for fragment of mass 110. In the same way the level density parameters were obtained for fission fragment masses 90 through 157. A new evaluation is needed. This can only be done with the help of the authors. If new measurements would be considered, they should be coordinated by the IAEA.

1.1.2 Non-Neutron Data for Standards

Alpha-Particle Emission Probabilities of ^{237}Np

G. Bortels, D. Mouchel, R. Eykens

There is an increasing interest in ^{237}Np, because, together with ^{99}Tc, it is one of the most important radionuclides remaining in nuclear waste even after long-term storage(1).

The objective of the work was to make a contribution to the reduction of the large uncertainties on the alpha-particle emission probabilities found in the literature. For a long time the request for an accuracy of 1 % for the emission probabilities of the major alpha-particle emission could not be fulfilled(2). Evaluated data are quoted with an uncertainty of about 20 %.

The measurement programme was carried out in collaboration with CIEMAT Madrid, AERE Harwell and Canberra Semiconductor NV Olen.

Sources of about 70 Bq activity were produced on glass discs by sublimation in vacuum at CBNM and at AERE. The ^{237}Np materials used were of two different origins. Highly enriched ^{240}Pu was added as an internal energy reference.

Two sources were measured in a solid angle of 1 % of 2π sr using a PIPS detector of 50 mm^2 active area. Four spectra of 7.1 10^5 to 1.4 10^6 events were obtained with a resolution of 9 keV and an energy scale of 0.645 keV/channel. In order to allow for long-term drift and to check for possible anomalies during counting 412 runs of four hours each were made. The position of the major peak in these spectra was fitted for that purpose.

Energy summing of alpha particles and conversion electrons was reduced by a factor between 7 and 20 by employing a 2 kG magnetic field between the source and the detector. Background counts were negligible.

The spectra were analyzed at CBNM and CIEMAT using two different fitting models (3,4). A typical spectrum is shown in Fig. 6. The uncertainties were obtained from an analysis of covariances in the fitting and include, where necessary, a contribution for the tailing subtraction. Preliminary results are listed in Table 2.

---

(1) M. Sakanoue, Radiochim. Acta 42 (1987) 103
(2) Decay Data of Transactinium Nuclides, Technical Report Series N° 261, IAEA, Vienna (1986)
(3) G. Bortels and P. Collaers, Appl. Radiat. Isot., Int.J.Radiat.Appl. Instrum. Part A 38 (1987) 831
(4) E. Garcia-Toreño and M.L. Aceña, Nucl. Instrum. Methods 185 (1981) 261

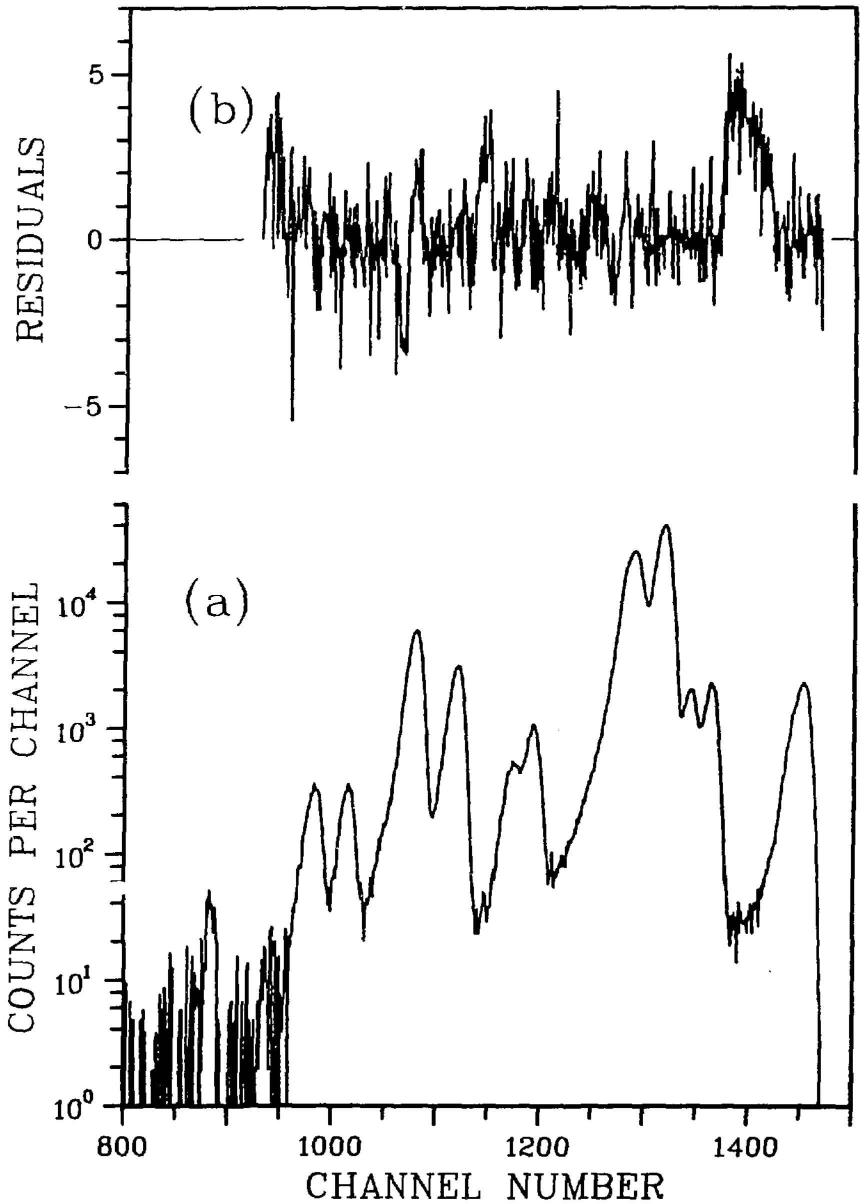

Fig. 6. (a) Alpha-particle spectrum of ^{237}Np after tailing subtraction; (b) Spectrum of the residuals after fitting in units of the standard deviation for the counts in the channels.

Table 2. Preliminary results of the measured alpha-particle energies and emission probabilities of ^{237}Np.

Energy [keV]	Emission Probability	Standard deviation
4513	0.00039	0.00004
4577	0.0040	0.0002
4598	0.0039	0.0002
4639	0.0643	0.0004
4665	0.0342	0.0005
4698	0.0054	0.0003
4711	0.0119	0.0005
4766.5	0.0958	0.0031
4771	0.2277	0.0059
4788	0.4776	0.0029
4804	0.0205	0.0004
4817	0.0247	0.0003
4867	0.0051	0.0004
4873	0.0242	0.0007

The 59.5 keV γ-Ray Emission Probability of ^{241}Am

B. Denecke, W. Bambynek

The radionuclide ^{241}Am is widely used as γ-ray source for the efficiency calibration of photon spectrometers. According to a recent assessment the accuracy of the emission probability of the 59.5 keV gamma rays is still not better than 1 % and the requirement of 0.2 % is not yet fulfilled[1]. To deduce the γ-ray emission probability both the disintegration rate and the γ-ray emission rate have to be determined.

The 59.5 keV γ-ray emission rate was measured with a specially designed windowless 4π-CsI(Tl)-sandwich spectrometer, which was developed as an "absolute" photon counter with almost 100 % detection efficiency. Uncapsulated detectors were used and particular care was taken by optimizing the counting geometry. As a result, absorption and scattering could be minimized. The accuracy obtained for the γ-ray emission rate is typically about 0.4 %.

[1] Decay Data of Transactinium Nuclides, Technical Report Series N° 261, IAEA, Vienna (1986), p. 9

The disintegration rates of the sources used were obtained from measurements of the alpha-particle emission rates in defined low solid angles. The accuracy of this method is 0.1 %.
The ratio of these two quantities, the γ-ray emission rate and the disintegration rate, is the 59.5 keV γ-ray emission probability. Special care has been taken to account for the contributions of the coincidence summing in the 59.5 keV peak. The obtained result is compared with other published values as shown in Table 3. It is significantly higher than some previously measured and also than the recently evaluated value. There are two groups of values reported in the literature. Consequently, further research is needed, either by new evaluations or measurements.

Table 3. Published values of the 59.5 keV γ-ray emission probability, P_γ, of ^{241}Am

P_γ [%]	Detector	Reference[a]
40.0 ± 0.15	PC	Beling et al. (1952)
35.9 ± 0.6	NaI(Tl)	Magnusson (1957)
34.6 ± 0.7	NaI(Tl)	McIsaac (1964)
38 ± 6	NaI(Tl)	Michaelis (1965)
35.3 ± 0.6	NaI(Tl) well	Peghaire (1969)
36.3 ± 0.4	NaI(Tl) well	Legrand et al. (1975)
35.5 ± 0.3	4π NaI(Tl)	Plch et al. (1976)
35.82 ± 0.12	NaI(Tl) well	Hutchinson and Mullen (1983)
36.36 ± 0.17	4π CsI(Tl)	Denecke (1987)
35.9 ± 0.4	- [b]	Bambynek (1986)

[a] W. Bambynek (1986), in Decay Data of Transactinium Nuclides, Technical Report Series No. 261, (IAEA, Vienna) p. 128.
J.K Beling, J.O. Newton and B. Rose (1952), Phys. Rev. 86, 797.
B. Denecke (1987), Appl. Radiat. Isot. A, 38, 823.
J.M.R. Hutchinson and P.A. Mullen (1983), Int. J. Appl. Rad. Isot. 34, 543
J. Legrand, J.P. Perolat, C. Bac and J. Gorry (1975), Int. J. Appl. Rad. Isot. 26, 179.
L.B. Magnusson (1957), Phys. Rev. 107, 161.
L.D. McIsaac (1964), IDO Report 17052, p. 31.
W. Michaelis (1965), Z. Phys. 186, 42.
A. Peghaire (1969), Nucl. Instrum. Methods 75, 66.
J. Plch, J. Zderadicka and L. Kokta (1976), Czech. J. Phys. B26, 1344.

[b] evaluated.

Radionuclide Data

W. Bambynek

The available nuclear- and associated atomic-data sources frequently used in radionuclide measurements were critically reviewed. Compilations and evaluations from the following fields were considered: nuclear structure and radioactive decay, alpha particles, nuclides decaying by electron capture, gamma rays, internal conversion, and associated atomic physics. An invited lecture "Radionuclide Data" was given at the First International Summer School on Low-Level Measurements and their Applications to Environmental Radioactivity, La Rábida, Spain.

Evaluations of X- and γ-Ray Emission Probabilities

W. Bambynek

In the frame of an IAEA Coordinated Research Project (CRP) on X- and γ-Ray Standards for Detector Efficiency Calibration the X-ray emission probabilities of the following radionuclides selected by the CRP members[1] were evaluated: ^{51}Cr, ^{54}Mn, ^{55}Fe, ^{57}Co, ^{58}Co, ^{65}Zn, ^{75}Se, ^{85}Sr, ^{88}Y, $^{93}Nb^{m}$, ^{109}Cd, ^{111}In, ^{125}I, ^{137}Cs, ^{133}Ba, ^{139}Ce, ^{152}Eu, ^{154}Eu, ^{198}Au, ^{203}Hg, ^{207}Bi.

---

[1] P. Christmas, A.L. Nichols and A. Lorenz, INDC(NDS)-196/GE (1987)

1.2 NUCLEAR DATA FOR FISSION TECHNOLOGY

In the field of nuclear data for fission technology the effort was concentrated on two areas : continuation of measurements and analysis of actinide data in the subthermal neutron energy range, and the measurements in connection with the NEANDC task force on the 1.15 keV resonance in ^{56}Fe. Besides these main items, work continued on the analysis of total and radiative capture cross-sections of the chromium isotopes. Excitation functions have been determined for a series of structural materials.

1.2.1 Neutron Data of Actinides

Fission Cross-Section Measurements at Low Neutron Energies

C. Wagemans*, P. Schillebeeckx*, A. Deruytter, R. Barthélémy, J. Van Gils*
(European High Priority List NEACRP-A-568, NEANDC-A-180)

A simultaneous analysis has been done of the previously performed ^{233}U, ^{235}U and $^{239}Pu(n,f)$ cross-section measurements at GELINA with low energy

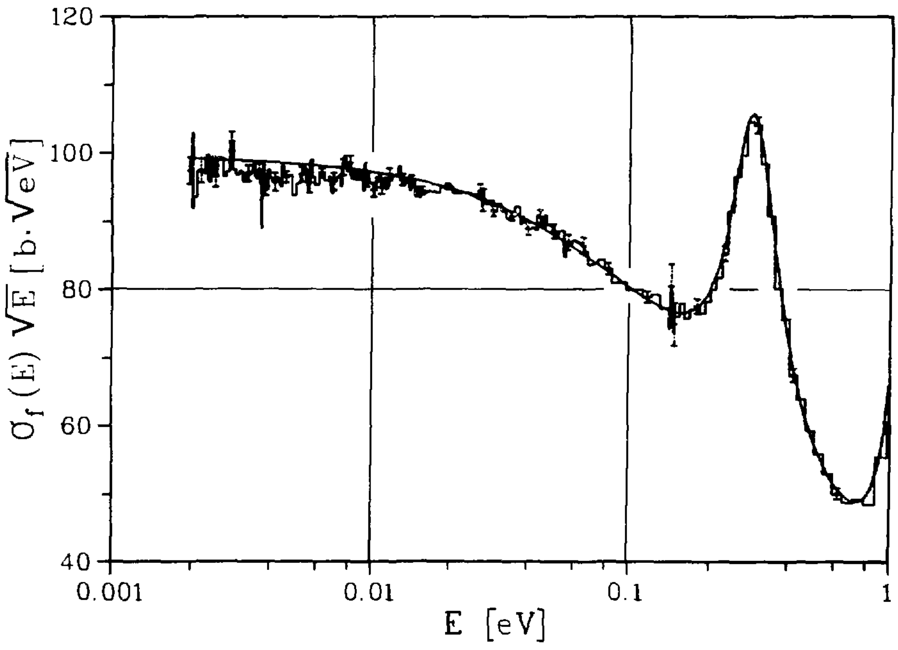

Fig. 7. The measured fission cross-section shape for ^{235}U compared to ENDF/B-5 (continuous line) in the neutron energy range from 2 meV to 1 eV

---

* SCK/CEN, Mol, Belgium

neutrons. In all cases, the neutron flux distribution was determined using the $^{6}Li(n,\alpha)T$ reaction. The present results considerably improve the σ_f-data base in the neutron energy region between 2 meV and 1 eV, where the available data are generally scarce and/or inaccurate. As a typical result, the $^{235}U(n,f)$ cross-section values obtained from the present experiments are shown in Fig. 7 together with the evaluated ENDF/B-5 file. Within the experimental error, the experimental data and the evaluated file agree, although the experimental data below 10 meV indicate that σ_f goes faster to a 1/v shape than believed before. These results also allow more accurate calculations of the Westcott g_f-factors, since these are strongly influenced by the shape of σ_f at very low neutron energies. From the present data the following values for g_f at T = 20.44 °C have been calculated: 0.994 ± 0.003 for ^{233}U; 0.976 ± 0.002 for ^{235}U; 1.055 ± 0.003 for ^{239}Pu. These values are in agreement with the best evaluated data.

Eta, η, of ^{235}U

H. Weigmann, J.A. Wartena, C. Bürkholz
(WRENDA 83/84 request N° 465 and European High Priority List NEACRP-A-568, NEANDC-A-180)

The experiment to measure the energy dependence of eta of ^{235}U has been described in the previous progress reports[1]. In short, a "black" ^{235}U sample which is sufficiently thick to absorb all neutrons with energies of interest is exposed to a neutron beam from the liquid methane moderator at the GELINA. The relative number of fission neutrons emerging from this sample is measured with a NE213 liquid scintillator with pulse shape discrimination. The neutron flux is monitored with two parallel plate proportional counters loaded with thin layers of ^{10}B and $^{235}UF_4$, or with ^{6}LiF and $^{235}UF_4$ in part of the runs. The definite measurement of the neutron flux shape at the position of the "black" U sample is done in separate runs by recording the yield of 480 keV γ rays from a thick ^{10}B slab replacing the "black" U sample.
A number of corrections have to be applied to the measured data: Apart from backgrounds, the dead time of the data acquisition system and of the pulse shape discrimination circuitry have to be considered. Further, the data have to be corrected for incomplete absorption and scattering of the incident slow neutrons in the "black" U sample and in the ^{10}B slab. The multiple scattering of the fission neutrons produced in the "black" U

---

(1) NEANDC (E) 272 "U" Vol. III Euratom, INDC(EUR) 020/G (1986), p. 25
NEANDC (E) 282 "U" Vol. III Euratom, INDC(EUR) 021/G (1987), p. 19

sample, the relative number of secondary fission events induced by these neutrons, and the fraction of all fission neutrons that are detected in the liquid scintillator, must be taken into account. The latter fraction depends on the spatial distribution of primary fission events within the"black" U sample, and thereby on the energy of the incident slow neutrons. Finally, the self-absorption of the 480 keV γ rays in the ^{10}B slab has to be considered. These corections have been calculated by approximate analytical expressions as well as by Monte-Carlo techniques. The first analysis of the present data mentioned in the previous progress report which seemed to indicate a flat shape of eta below 20 meV neutron energy, did not include these corrections, especially the multiple scattering of the produced fission neutrons, in a complete manner.

The energy dependence of eta of ^{235}U resulting from the measurements at GELINA and including all above-mentioned corrections, is shown in Fig. 8 together with the "reference shape" as well as the modification proposed by Santamarina et al.[1]. The experimental data have been normalized to an average value of 2.075 between 20 and 30 meV neutron energy.

The error bars as shown in Fig. 8 include both, statistical as well as systematic uncertainties. However, the largest contribution is due to the

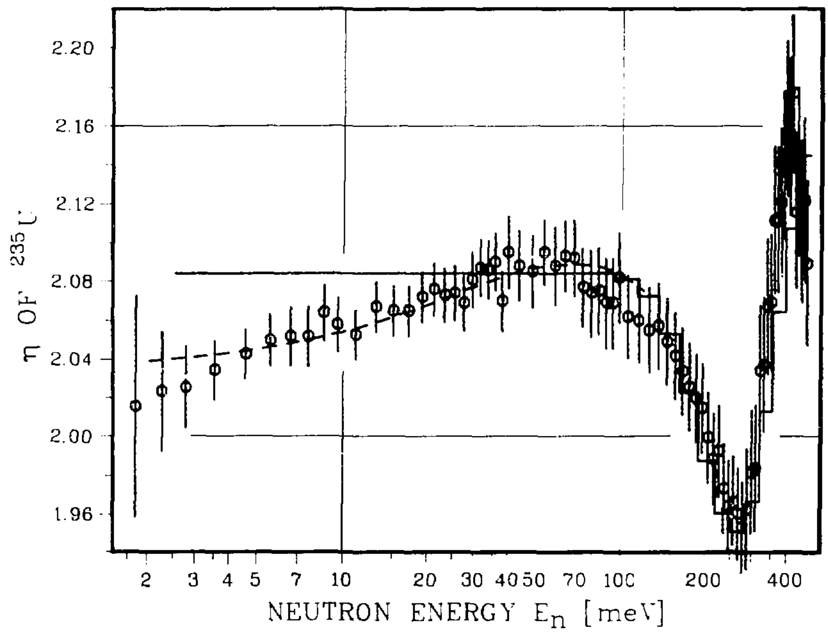

Fig. 8. The measured energy dependence of eta of ^{235}U compared to the reference shape (—) and the modification (---) proposed by Santamarina et al. [1]

---

[1] A. Santamarina, C.Golinelli, L. Erradi, ANS Topical Meeting on Reactor Physics, Chicago 1984

uncertainties in the determination of backgrounds (at low energies) and in the calculation of the correction factors (at high energies).
Thus the data uncertainties are highly correlated.

Determination of the Shape of the $^{235}U(n,f)$ Cross Section with Very Cold Neutrons

C. Wagemans*, A. Deruytter, R. Barthélémy, W. Mampe**, P. Ageron**, A. Michaudon**
(European High Priority List NEACRP-A-568, NEANDC-A-180)

Complementary to the previous experiments, the shape of the $^{235}U(n,f)$ cross section has been determined for very low energies at the Very Cold Neutron Source of the ILL at Grenoble. For this purpose a slow chopper has been installed at the end of the very cold neutron guide. An 11 μg/cm² $^{235}UF_4$ layer and a 3 μg/cm² ^{6}LiF layer were mounted back-to-back in a vacuum chamber at a distance of 58.1 cm from the chopper. The $^{235}U(n,f)$ and the $^{6}Li(n,\alpha)T$ particles were detected in a low geometry with surface barrier

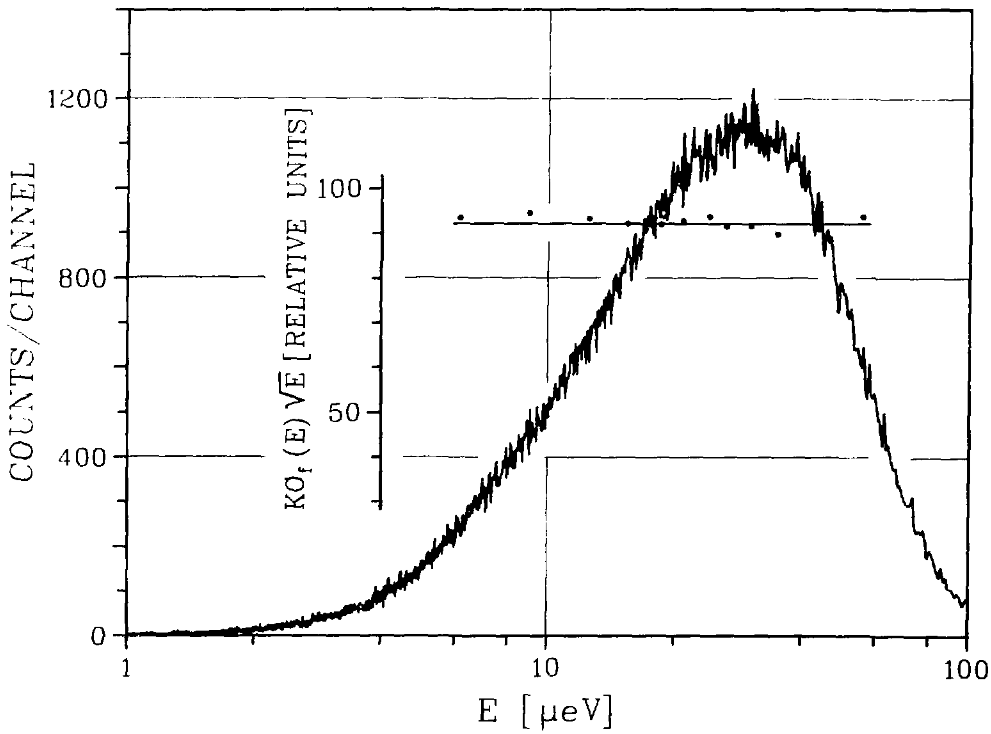

Fig. 9. The measured neutron flux spectrum at the Very Cold Neutron Source of ILL. Dots give values of $K\sigma_f\sqrt{E}$ (relative units) for ^{235}U, in the neutron energy range from 6 μeV up to 60 μeV

---

* SCK/CEN, Mol, Belgium
** ILL, Grenoble, France

detector. From these counting-rates values of $k\sigma_f(E)\sqrt{E}$ were calculated (Fig. 9). Within the precision, these results do not show a significant deviation of the ^{235}U fission cross section from a 1/v shape. So it is believed that a 1/v extrapolation of σ_f from 2 meV down to zero energy, as generally applied, is justified.

Fission-Fragment Mass and Energy Distributions for the Spontaneous Fission of Plutonium Isotopes

C. Wagemans*, P. Schillebeeckx*, A. Deruytter, R. Barthélémy

In the frame of a systematic investigation of the fission-fragment mass and energy distributions of plutonium isotopes, the spontaneously fissioning isotopes $^{238,240,242}Pu$ have been studied previously relative to the $^{239}Pu(n_{th},f)$ reaction. For these isotopes, strong neutron shell effects were observed, which appeared to be very enhanced when a closed shell occured in both the light and the heavy fission fragment. It is expected that the probability for such combinations be particularly high for ^{236}Pu. Thus, a measurement of the spontaneous fission reaction of that plutonium isotope has been performed. The obtained data are being analysed.

1.2.2 Neutron Data of Structural Materials

Experimental Excitation Function for $^{52}Cr(n,2n)$

H. Liskien, M. Uhl**, H. Vonach**, M. Wagner**, G. Winkler**

The reaction $^{52}Cr(n,2n)$ leads to the well-known nuclide ^{51}Cr with a half-life of 27.7 days. Using the activation method and monoenergetic neutrons from the $T(d,n)^4He$ reaction the excitation function has been determined in cooperation with IRK Vienna. The neutron fluence at the 24 sample positions were determined relative to the n-p elastic scattering process employing a recoil proton telescope and relying on the well-known angular distribution for the neutrons from the T(d,n) reaction. Resulting preliminary cross sections are consistent with unpublished results from a cooperation between IRK Vienna and Kossuth University Debrecen at ~ 14 MeV and consistent with recent theoretical calculations; they disagree above 15.2 MeV with the results recently published by S.K. Ghorai et al.[1]. At present scattering and absorption corrections are performed.

---

* SCK/CEN, Mol, Belgium
** IRK Vienna, Austria
(1) S.K.Ghorai, J.R. Williams, W.L. Alford, J. Phys G : Nucl. Phys. 13 (1987) 405

(n,p) and (n,α) Excitation Functions for Molybdenum Isotopes

H. Liskien, S.M. Qaim*, R. Wölfle*

Fifteen molybdenum samples (20 mm ∅ 5 mm) of natural isotope composition have been irradiated for 63 hours with monoenergetic neutrons from the $T(d,n)^4He$ source reaction covering the energy range from 12.6 to 19.6 MeV. The neutron fluence at the sample position has been determined in two independent ways. Firstly by sandwiching the samples between aluminium foils and determining the ^{24}Na activities, thus relying on the $^{27}Al(n,\alpha)$ standard cross section. Secondly by employing a recoil proton telescope, thus relying on the H(n,p) standard scattering cross section. Good agreement between the two sets of fluence results was observed. Activity determinations were performed at KFA Jülich. Work will at least yield results on the (n,p) reactions for ^{92}Mo, ^{95}Mo and ^{96}Mo and the (n,α) reactions for ^{92}Mo, ^{98}Mo, and ^{100}Mo. Data analysis is on the way.

Excitation Functions of $^{93}Nb(n,2n)^{92m}Nb$, $^{93}Nb(n,\alpha)^{90m,g}Y$, $^{139}La(n,\alpha)^{136}Cs$ and $^{181}Ta(n,p)^{181}Hf$ Reactions in the Energy Range of 12.5-19.6 MeV.

R. Wölfle*, A. Mannan* S.M. Qaim*, H. Liskien, R. Widera

Cross sections were measured for the $^{93}Nb(n,2n)^{92m}Nb$, $^{93}Nb(n,\alpha)^{90m,g}Y$, $^{139}La(n,\alpha)^{136}Cs$ and $^{181}Ta(n,p)^{181}Hf$ reactions in the energy range of 12.5-19.6 MeV. Use was made of the activation technique in combination with high-resolution γ-ray spectroscopy, except for the product ^{90g}Y where radiochemical separation and β counting were applied. The neutron fluence rates were determined using two independent methods, viz. proton recoil telescope and $^{27}Al(n,\alpha)^{24}Na$ monitor reaction. An appraisal of the available cross section data for the five investigated processes was carried out. Due to its relatively high importance as a dosimetry reaction an evaluation of the $^{93}Nb(n,2n)^{92m}Nb$ excitation function based on the most recent data is recommended. For the other reactions the measurements furnish an extended data base. A comparison of the experimental data with values calculated from the semi-empirical code THRESH has been made. The code predicts unknown activation cross sections only with partial success. This work has meanwhile been finalized and accepted for publication in Int. Radiat. Appl. Instrum. Part A.

* KFA, Jülich, Germany

The Weighting Function of a C_6D_6 Detector and the 1.15 keV Neutron Resonance of ^{56}Fe

F. Corvi, G. Fioni*, F. Gasperini, P.B. Smith**
(relevant to 1.15 keV ^{56}Fe Task Force of NEANDC)

A paper on the experimental determination of the weighting function of a neutron capture detector in the range 0.5 - 9 MeV has been recently published. Contributed papers on the same subject have also been presented at the International Symposium on Capture γ-Ray Spectroscopy, Leuven, 1987 and at the International Conference on Neutron Physics, Kiev, 1987.
The results of these published works do not exhaust the present topics since a satisfactory explanation of the observed effect is still missing. In order to investigate in particular why the measured characteristics of the detectors are so different from predictions, research has been continued on two main lines :
(1) The resonance at E_p = 0.62 MeV for the reaction ^{30}Si(p,γ) was chosen as a source of almost monochromatic high-energy γ rays. In fact, the ^{31}P compound state excited by this resonance decays to the ground state with a 95% branching ratio via a transition of energy E_γ = 7.898 MeV. The efficiency, E, of the C_6D_6 liquid scintillator for this γ ray was measured with a calibrated ^{60}Co source by comparing the ratio of the counting rates of the scintillator for the two γ ray sources to the corresponding ratio of the full peak areas in the amplitude spectra of a coaxial Ge detector. The relative full peak efficiency of the latter detector for the transitions under investigation could be determined by measuring the decay of the ^{30}Si(p,γ) resonance at E_p = 1.398 MeV, dominated by the two-step cascade consisting of the 7.383 and the 1.266 MeV γ rays, with well known intensities. The low energy transition can very well represent the two ^{60}Co lines since its energy is almost equal to their average. The difference in efficiency between 7.383 and 7.898 MeV was estimated from data of the other ^{30}Si resonances. After subtracting the contribution of the other γ rays present in the decay of the E_p = 0.62 MeV resonance, the result for C_6D_6 is $\varepsilon(7.90)/\varepsilon(1.25) = 1.02 \pm 0.05$. This value agrees with the results of the coincidence method confirming the approximately constant behaviour of the efficiency as a function of the energy.

---

* EC Fellow
** University of Groningen, Groningen, The Netherlands

The absolute values of the efficiency could also be determined since the ^{60}Co source used was calibrated to better than 1 %; in particular, it was found that the measured efficiency at 1.25 MeV agrees within the errors with that calculated simply from the known cross sections. In additional runs the C_6D_6 scintillator was replaced by other detectors and similar intercomparison measurements were carried out. The results are summarized in Fig. 10 where the relative difference between the experimental and calculated efficiency for the 7.898 MeV transition is plotted versus the calculated intrinsic efficiency P of each detector.

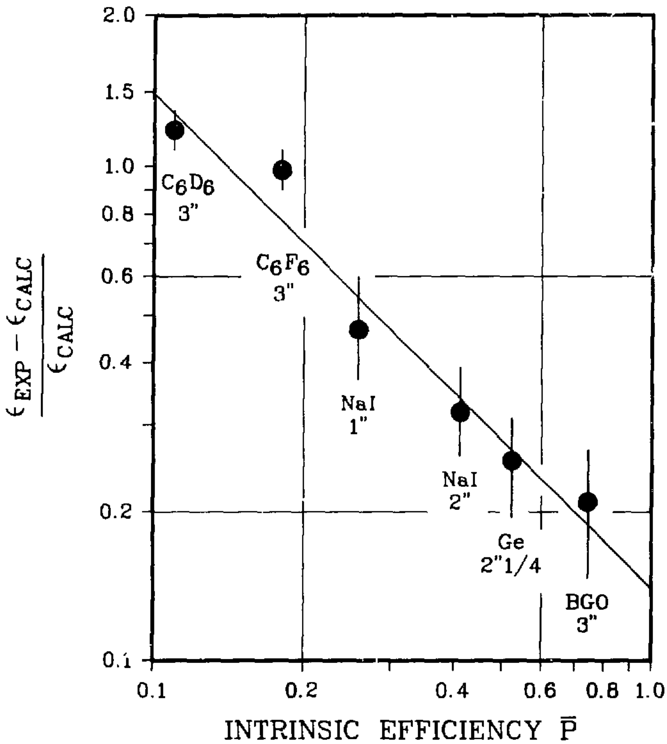

Fig. 10. Relative difference between experimental and calculated efficiency plotted versus the intrinsic efficiency $\bar{P}$. Detector composition and thickness are given beneath each point. The full line is a fit of the slope $1/\bar{P}$ for the γ ray of energy E_γ = 7.898 MeV

The intrinsic efficiency is defined as $\bar{P} = \langle 1-\exp(-\mu d) \rangle$, where μ is the total attenuation coefficient and d is the path-length through the detector. The plot shows that the effect found in the C_6D_6 scintillator, namely a measured efficiency larger than expected for high-energy γ rays, is common to all detectors. Moreover, by fitting the data points with a function of the type $Y = aX^b$, one gets b = 0.99±0.11. in good agreement with unity. Since $\varepsilon_{calc} = (\Omega\bar{P})/4\pi$, where Ω is the source solid angle subtended by the entrance face of each detector, one can write $(\varepsilon_{exp} - \varepsilon_{calc}) \sim \Omega/4\pi$. It means that the "unknown" radiation responsible for the difference between experimental and calculated counting rate has an efficiency independent of $\bar{P}$. As a consequence, it cannot consist of γ rays but rather of electrons and positrons which have of course a 100% efficiency. Tests to check this hypothesis are on the way.

(2) Improved Monte Carlo calculations of detector characteristics have been carried out, in close collaboration, by F. Perey of ORNL who was employing the EGS4 code from the Stanford Linear Accelerator Laboratory. From this exercise it became apparent that the old codes used for calculating the weighting function were inadequate both because of a lack of an accurate description of electron and gamma transport and because they were not designed to include in detail the effect of the environment. In particular an important role is played by the sample (or the backing, in case of (p,γ) reactions) acting as a source of high energy electrons and positrons which are detected by the liquid scintillator with an efficiency much larger than that of the primary γ rays.

As a result of all this, the difference between the measured values of response functions and efficiencies and those calculated by EGS4 is now smaller than was stated before, when the old code for the weighting function was still used. However, up to now the agreement is not yet satisfactory, moreover the weighting function calculated with EGS4 for the neutron capture setup does not reproduce the transmission value of the 1.15 keV ^{56}Fe resonance. The exercise is continuing and it is now too early to draw any definite conclusion.

1.2.3 Matters Related to Fission Technology

Measurements of the Cross Section of the Reaction $^{93}Nb(n,n')^{93m}Nb$ at $E_n \sim 7.9$ MeV by Activation.

M. Wagner*, G. Winkler*, H. Vonach*, H. Liskien.

The reaction ^{93}Nb(n,n')^{93m}Nb is particularly important as long-term activation monitor in reactor dosimetry due to the long half-life of the produced ^{93m}Nb isomer [$T_{\frac{1}{2}}$ = (16.13 ± 0.10) a] and its low reaction threshold (~ 31 keV).

In order to establish the excitation function of the dosimetry reaction ^{93}Nb(n,n')^{93m}Nb more precisely, an activation measurement close to 8 MeV neutron energy seemed to be very informative since no other experimental result for the production of the 30.7 keV isomer of Nb in that particular energy region could be found in the literature. An irradiation was carried out at CBNM Geel. The reaction D(d,n)^{3}He was used as a neutron source employing a deuterium gas cell. The incident deuteron energy was ~ 5.09 MeV where a contribution of deuterium break-up neutrons has not to be taken into account.

A niobium foil, ~ 0.13 mm thick and 20 mm in diameter was used as sample. A distance of only 6 mm between this foil and the front of the gas cell (at 0° relative to the d$^+$ beam) was chosen. In an irradiation of ~ 60 hours a total neutron fluence of ~ $5 \cdot 10^{12}$ cm^{-2} at the sample position has been achieved which resulted in a ^{93m}Nb activity of 0.8 - 1.0 counts per minute. A background run with another foil lasting for ~ 29 hours was performed with the gas cell filled with helium instead of deuterium.

A ^{238}U-fission chamber in a back-to-back geometry with the niobium foil served for the neutron fluence determination. The mass calibration of the used ^{238}U reference layer revealed some inconsistency. Therefore, a separate irradiation experiment with 14.8 MeV neutrons, employing a 200 keV Cockcroft-Walton generator, was performed at IRK Vienna. In this experiment the mass of the ^{238}U deposit used as the reference fluence monitor in an ionization chamber was determined relative to the mass of an aluminium foil, thus relying on the ^{238}U(n,f)/^{27}Al(n,α) cross section ratio at this energy. Additionally, low geometry α-particle counting was performed at CBNM Geel.

The ^{93m}Nb activities induced in the niobium foils were measured detecting the niobium K X-rays by means of a Si(Li) detector.

---

* IRK, Vienna, Austria

Effects of the sample extension and self attenuation were determined experimentally. Due to the very low K X-ray count rates to be measured special attention had to be paid to K X-ray fluorescence induced in the sample by background radiation.

1.3 NUCLEAR DATA FOR FUSION TECHNOLOGY

Double-Differential Neutron-Emission Cross Sections for ^{7}Li

E. Dekempeneer*, H.Liskien, L. Mewissen** and F. Poortmans**

Double-differential neutron-emission cross sections for the $^{7}Li(n,xn)$ reaction have been determined for average emission angles of 24, 40, 60, 90, 120, and 150 deg. The incident neutron energy was in the range from 1.6 to 13.8 MeV. The cross sections were measured using an electron linear accelerator as a pulsed white neutron source. Elastically scattered neutrons and neutrons scattered via the 0.48 MeV state are treated as one single group. Inelastic scattering cross sections are obtained for the 4.63 and 6.54 MeV states. For this purpose, the underlying neutron continuum coming from competing tritium-producing reactions (three-particle breakup and sequential two-step reaction via the ^{5}He ground state) is estimated using simple physical model calculations. The data were compared with recent evaluations. This work has been finalized and published.

New measurements on ^{7}Li are planned as soon as the construction of a new accelerator target is finished. This target will consist of a uranium-beryllium mixture and will produce a harder neutron spectrum than the presently used uranium target. There are two reasons for a remeasurement. First, to expand the data set beyond 14-MeV primary neutron energy toward 16 MeV. In this energy region, all recent evaluations still rely on optical model extrapolations with practically no experimental data for comparison. Second, the double-differential neutron-emission data obtained in this study stop at a secondary neutron energy threshold of 1.5 MeV. At lower energies difficulties with an unstable pulse-shape discrimination arised. It is expected to lower this secondary energy threshold to 0.7 MeV by implementing an on-line control of the pulse-shape discrimination properties.

Experimentally Determined Excitation Function for the $^{9}Be(n,t)$Reaction.

H. Liskien, R. Widera, S.M. Qaim*, R. Wölfle*

For the first time, an experimentally determined excitation function for tritium production from beryllium has been obtained. Beryllium samples

---

* Philips N.V., Eindhoven, The Netherlands
** SCK/CEN, Mol, Belgium

were irradiated with well-known fluxes of monoenergetic neutrons in the 12.86 to 19.57 MeV energy range and the induced tritium was quantitatively extracted and counted. The results disagree with the JEF-1 prediction but show a remarkably good agreement with JENDL-3/PR2 and a recent evaluation from the Los Alamos National Laboratory, both based on 14 MeV values and theoretical calculations. This work has been finished and published.

Double Differential Neutron Emission Cross Sections for the $^{9}Be + n$ Reactions

E. Dekempeneer **, L. Mewissen***, F. Poortmans***, H. Weigmann

Beryllium is a candidate neutron multiplier for the blanket of a fusion reactor. Calculating the tritium breeding rate in the blanket requires a detailed knowledge of the energies and angular distributions of the neutrons emitted from beryllium through the elastic and various inelastic neutron channels.

A first series of measurements of double-differential neutron-emission cross sections has been done at GELINA, covering an incident energy range from 1.5 to 9 MeV. The measurements have been discontinued temporarily and will be taken-up again and extended to higher energies when the U-Be target will be operational.

Development and Tests of an Alpha-particle Telescope with Sub-nanosecond Timing

E. Wattecamps, G. Rollin

To measure rather small (n,α) cross sections in the presence of a large background a new telescope was designed. The detector system is specific, redundant and has still a reasonable efficiency. The telescope is made of two identical multi-wire-parallel-plate-avalanche counters (MWPPAC) and a thin pilot-U scintillator. One MWPPAC is in front of the scintillator, and the distance between the first and the second MWPPAC is 18 cm. Each MWPPAC has a circular multiwire anode plane of 5 cm diameter (gilded tungsten wires of 20 μm diameter, every 0.8 mm) between two polycarbonate cathode

---

* KFA, Jülich, Germany
** Philips N.V., Eindhoven, The Netherlands
*** SCK/CEN, Mol, Belgium

foils of 150 μg/cm^2. The distance between anode and cathode plane is 3.5 mm. The counting gas is isobutane at 4 mbar, in continuous flow, with pressure regulation to within 0.5 %. Each detector has a conventional, slow and fast electronic chain. The multiparameter data acquisition in incremental mode and in listing mode is performed with a ND6660 analyser.
The telescope and its acquisition system provide : (1) a triple coincidence, (2) the energy loss in each MWPPAC, (3) the alpha particle energy by the pulse-height in the scintillator and (4) the alpha particle energy by the time of flight between the first MWPPAC and the scintillator.
Test measurements were done with monoenergetic alpha-particles from ^{241}Am and subsequently with reduced energies by inserting thin foils between the source and the telescope.The test measurements gave the following results:

- the time resolution of a single MWPPAC is 570 ps for alpha-particles between 1 and 5 MeV,
- the time resolution of the scintillator is smaller,
- the energy resolution of the MWPPAC is 55 %, the pulse-heights well above noise,
- the energy resolution of the pilot-U scintillator is 19 %,
- the above features, in particular the time resolution, were observed during many days, thus demonstrating satisfactory long term stability,
- repeatedly the system was shut down and restarted with satisfactory characteristics achieved in a reasonable time.

The telescope was installed recently in front of the target with the neutron burst width of 360 ps. Tests under accelerator condition with neutrons from the D(d,n) reaction and a nickel sample have been started.

Measurements of Double-Differential (n,α) Cross Sections

E. Wattecamps
(Wrenda request Nrs 801147, 78106, 781064)

In the past measurements of double-differential (n,α) cross sections of natural nickel and copper were made in the 5 to 10 MeV neutron energy range in steps of 0.5 MeV. In the case of copper agreement between experimental data obtained by various techniques but a weaker dependence on neutron energy than predicted by evaluated files is found. In the case of nickel the available experimental and evaluated data are discrepant. To solve these discrepancies measurements of (n,α) cross section ratios on the main single isotopes were performed, namely ^{60}Ni to ^{58}Ni, ^{63}Cu to ^{58}Ni and ^{65}Cu to ^{58}Ni, between 5 and 10 MeV and at 14 MeV neutron energy. Measured (n,α) cross section ratios of ^{60}Ni to ^{58}Ni are shown in Fig. 11 together with the ratios deduced from the evaluations JENDL-1 and JENDL-2, a recent calculation of ORNL, and experimental data obtained elsewhere. The ratios are larger than those deduced from the JENDL evaluations, but are, within the uncertainty margins, still consistent with the data of Graham et al.[1]. The recent model calculations of Hetrick et al.[2] of ORNL agree best. Measured (n,α) cross section ratios of ^{63}Cu to ^{58}Ni are given in Fig. 12. At 8 MeV there is good agreement with a ratio deduced from independent measurements of ^{63}Cu(n,α) by Paulsen[3] and ^{58}Ni(n,α) measured

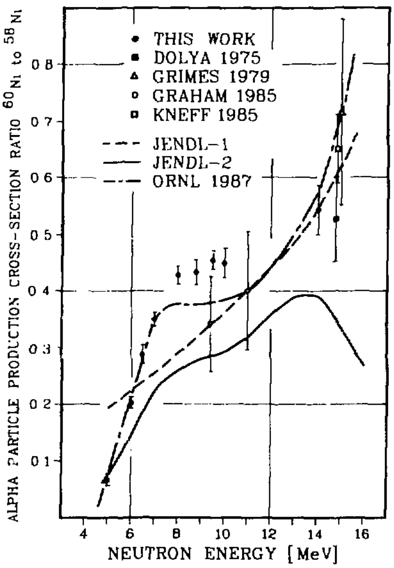

Fig. 11. Measured alpha-particle production cross-section ratio of ^{60}Ni to ^{58}Ni together with evaluations and calculations

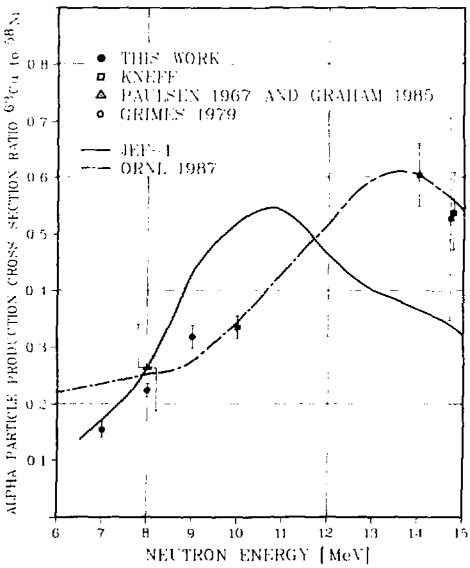

Fig. 12. Measured alpha-particle production cross-section ratio of ^{63}Cu to ^{58}Ni together with evaluations and calculations

---

(1) S.L. Graham et al., Nucl. Sci. Eng. 97 (1987) 60
(2) D.M. Hetrick et al., ORNL/TM-10219 (1987)
(3) A. Paulsen, Nukleonik 10 (1976) 91

by Graham et al.. Again the recent model calculations of Hetrick et al. agree best with the present experimental data. A cross section ratio curve was also deduced from the $^{58}Ni(n,\alpha)$ and $^{nat}Cu(n,\alpha)$ evaluations of JEF-1. Starting from $^{nat}Cu(n,\alpha)$ a small contribution of $^{65}Cu(n,\alpha)$ had to be subtracted. A more detailed analysis is in progress, which will provide double-differential cross sections (angular- and energy distributions).

1.4 SPECIAL STUDIES

Ground State Partial Radiative Widths of $^{28}Si + n$ Resonances

P.W. Martin*, L. Mewissen**, F. Poortmans**, J.A. Wartena, H. Weigmann

The data on neutron resonances in $^{28}Si+n$ described in the previous progress report[1], have been further analysed with respect to M1 and E2 radiative transition strengths. The total M1 strength detected in $^{29}Si+n$ is $B(M1) = 1.6\ \mu^2_0$ plus another possible $0.4\ \mu^2_0$ from a strongly radiating level with unknown parity at 11.499 MeV excitation energy. This is in contrast to the value of $B(M1) = 5.9\ \mu^2_0$ reported for ^{28}Si from inelastic electron scattering. Due to the decreasing sensitivity of the $^{28}Si(n,\gamma)$ experiment, additional M1 strength in ^{29}Si may have escaped detection above 11 MeV excitation energy, if it is strongly fragmented. However, a true reduction of M1 strength in ^{29}Si as compared to ^{28}Si may also result if the additional neutron in ^{29}Si occupies the $d_{3/2}$ state with a non-negligible probability, thus blocking spin flip transitions into this state.

E2 ground state transitions with partial widths of 0.1 and 0.25 eV have been observed from two $5/2^+$ resonances at about 9.5 MeV excitation energy. With reduced strengths of 5.04 and 10.76 e^2fm^4 they represent very strong E2 transitions, exceeding the empirical expectation value for E2 transitions in this mass range by factors of 2.3 and 5.2, respectively. Since besides the two observed E2 transitions there are eight additional $5/2^+$ resonances known in ^{29}Si from the total cross section analysis for which no ground state γ rays have been observed, the average $\Gamma_\gamma(E2)$ in ^{29}Si seems to be in rough accord with the empirical estimate.

Doorway Structure in $^{28}Si + n$ and $^{32}S + n$ Based on Discontinuities of the Level Spacing

G. Rohr and R. Shelley

In this study neutron resonance data of ^{28}Si and ^{32}S are used which have been recently obtained from the analysis of high resolution measurements

---

* Visiting scientist from the University of British Columbia, Vancouver, Canada

** SCK/CEN, Mol, Belgium

(1) NEANDC (E) 282 "U" Vol. III Euratom, INDC 021/G (1987), p. 39

performed at the GELINA. According to the level density systematics the calculated level density of doorway-states agrees with the experimental level density ρ_{ex} for nuclei with $A<35$ and the increase in ρ_{ex} at $A \approx 36$ indicates the transition to 3p-2h states. A similar increase should be expected for nuclei $A<35$ as a function of the excitation energy. A rise in the maximum analysed energy to 2.75 and 1.7 MeV for ^{29}Si and ^{32}S respectively would be helpful to demonstrate this:

Resonance data of ^{33}S : the s-wave resonance parameters of ^{33}S are plotted in Fig.13. The resonance energy is marked on the abscissa and its corresponding reduced neutron width is given on the ordinate. A brief inspection of the resonance energies points to an accumulation of resonances at 1.4 MeV. This behaviour can be expressed quantitatively by the different level spacings of 315 and 102 keV calculated in the energy intervals 0-1.05 MeV and 1.0-1.7 MeV, respectively. The increase in the level density by a factor of three indicates that the doorway resonances beyond 1.0 MeV are split into 3p-2h states. A threshold of $\Gamma_n° = 1.25$ eV seems to separate the doorway from the other resonances. Moreover, we assume that the smaller resonances close to the doorway resonance are 3p-2h states and that they belong to the same doorway structure. Then we calculate D_f, the average level spacing of 3p-2h resonances with respect to its doorway resonance, and the ratios $\Gamma f_H/(\Gamma f_D+\Gamma f_H)$ and $D_f/(\Gamma f_D+ \Gamma f_H)$, where Γf_D is the remaining doorway width and Γf_H is the sum of the widths spread into 3p-2h resonances. The sum $\Gamma f_D+ \Gamma f_H$ agrees with the decay width $\Gamma\uparrow$, a term which is used together with the spreading width $\Gamma\downarrow$ to describe the doorway structure when the doorway state is fully fragmented into hierarchy states. The results for the three doorway structures are included in Fig. 13 and their smooth variation with energy justifies the procedure used above. The first ratio increases monotonically and reflects an increase in the fragmentation with the excitation energy. The second ratio illustrates a sort of repulsion effect: the splitting of the fine structure resonances is proportional to the decay width of the doorway state and increases with excitation energy.

Resonance data of ^{29}Si : the s-wave resonance parameters of ^{29}Si are plotted in Fig. 14. The nine resonances are grouped into three doorway structures. Since the doorway resonance is only partly fragmented into states of higher hierarchy, as in the ^{33}S case, the doorways can be separated by a threshold of $\Gamma_n° = 6.5$ eV. The results of the ratios are included in Fig. 14 and show similar properties as the ^{33}S doorway structures: the fragmentation increases with the excitation energy and the

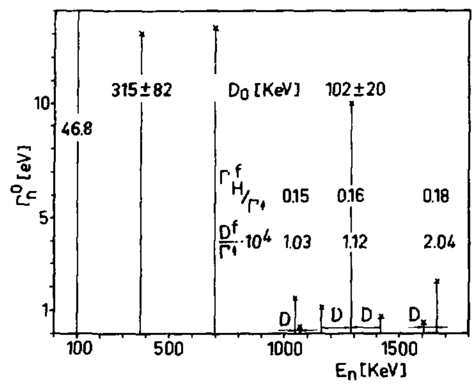

Fig. 13. *Resonance energies and reduced neutron widths for ^{33}S*

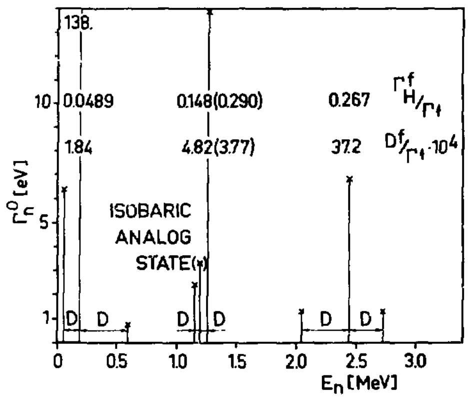

Fig. 14. *Resonance energies and reduced neutron widths for ^{29}Si*

splitting of the 3p-2h resonances is proportional to $\Gamma\uparrow$ and increases with energy. However this smooth behaviour is not observed if the resonance at 1.2 MeV is included (bracket values). This resonance has been assigned as an isobaric analogue state which is at least partly fed by electro-magnetic interaction. The explanation for this deviation underlines the above mentioned regularity of the properties of doorway structures.

In conclusion, the classical doorway effects described in the literature, are the same for electromagnetic and nucleon-nucleon interactions and are indicated by systematic changes in the width of resonances. In contrast the given examples of doorway states are indicated by discontinuities in the level density and the result of the resonance parameters point to a connection between the decay-width and the splitting of fine structure resonances. The amount of splitting is proportional to the spreading width and seems to indicate a level repulsion effect, caused by the two-body interaction in nuclei.

A possible explanation for the small spreading width of the doorway structures has been discussed during an oral presentation at the 6th International Sysmposium on Capture Gamma-ray Spectroscopy in Leuven 1987.

The $^{41}Ca(n,\alpha)^{38}Ar$ Reaction in the Resonance Region

C. Wagemans*, H. Weigmann, R. Barthélémy, J. Van Gils*

A gridded gas-flow ionization chamber has been put into operation, enabling a detection of the energy and the angular distribution of the alpha-particles emitted from the reaction $^{41}Ca(n,\alpha)$ in the resonance region. Corresponding measurements have been started and are being continued.

Ground State Partial Radiative Widths of $^{207}Pb + n$ Resonances and M1 and E2 strengths in ^{208}Pb

L. Mewissen*, F. Poortmans*, S. Raman**, J.A. Wartena, H. Weigmann

Analysis of the data on neutron resonances in $^{207}Pb+n$, described in the previous progress report has been finalized by investigating the electric quadrupole strength from identified $J^{\pi} = 2^{+}$ resonances. In Fig. 15 the distribution of the observed electric quadrupole strength, $B(E2)\uparrow$, is

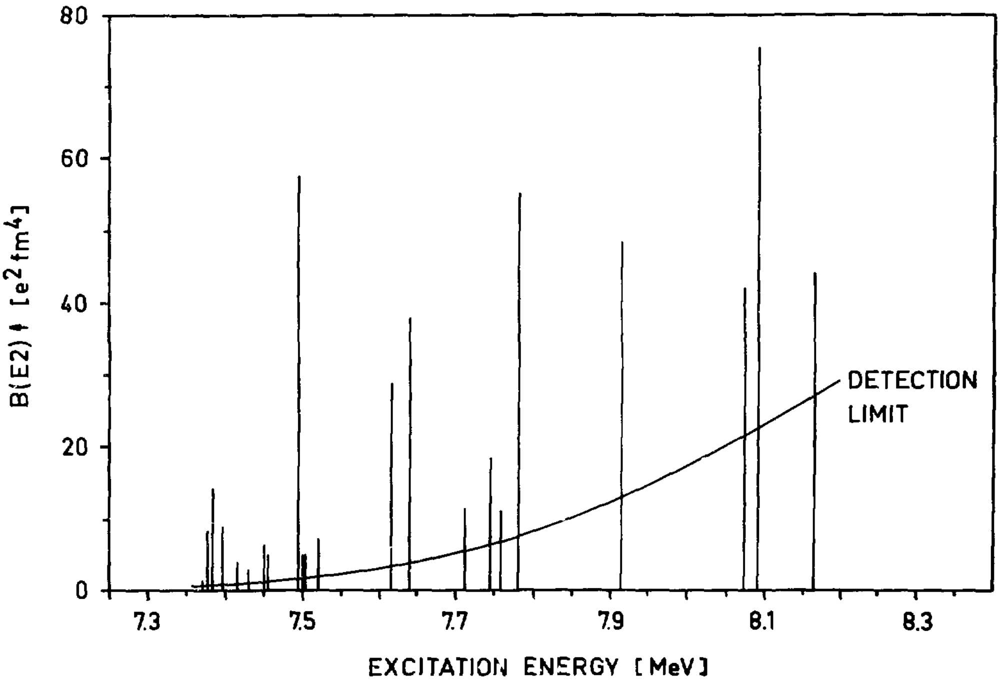

Fig. 15. Distribution of reduced electric quadrupole strength of $J^{\pi} = 2^{+}$ resonances.

* SCK/CEN, Mol, Belgium
** ORNL, Oak Ridge, Tenn., USA

shown. Above 800 keV neutron energy no 2^+ resonances could be identified. The experimental detection limit is also indicated. The energy-weighted sum of the observed E2 strength is

$$\Sigma\, E_\gamma\; B(E2)\uparrow /e^2 = 0.4\ \mathrm{MeV\,b^2}.$$

This corresponds to 4.9 % of the energy-weighted sum-rule for isoscalar E2 transitions. As seen from Fig. 15, the distribution of E2 strength in the energy range of the present analysis is rather uniform. This is in contrast to the apparent clustering of E2 strength reported in inelastic proton scattering.

Investigation of Intruder States Observed in Even Lead Isotopes

G. Rohr, R. Shelley

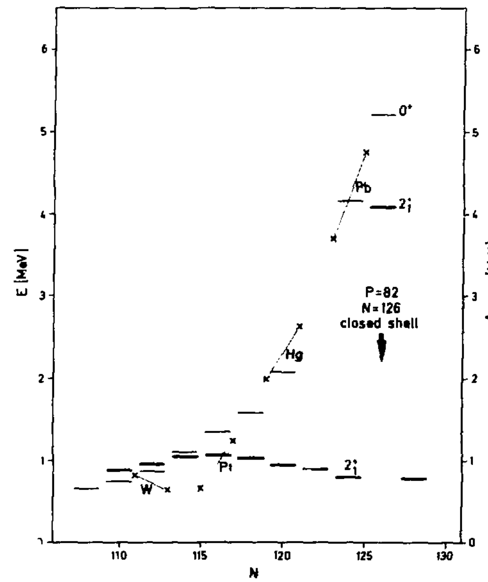

Fig. 16. Systematics of the 2^+ phonon and 0^+ intruder states for even mass lead isotopes and the ground state shift Δ_{shell} calculated from the level density systematics indicated by crosses

The study of intruder states has been extended to lead isotopes, for which the largest shift has been observed and the bound states of these nuclei have been examined extensively. In the present study for the first time resonances are used to investigate intruder states in lead. In Fig. 16 the 2^+ and the 0^+ states are presented as a function of the neutron number for even lead isotopes. The energy of the first 2^+ state, the one phonon state, is almost independent of neutron number. In contrast the behaviour of the 0^+ state shows a decreasing shift from an excitation energy larger than 5 MeV to values lower than 1 MeV, so that this state becomes the lowest excited state for neutron deficient nuclei.

These 0^+ states are called intruder states and their total shift amounts to more than 4.5 MeV. A part of this shift is caused by a change in the pairing energy[1].

---

[1] G. Rohr, Z. Phys A318 (1984) 299

A shift of states can be expected not only at lower energy but also for higher energies, for instance at neutron separation energy where a change in the level density should be observed. For masses around A=208 an enormous reduction in the level density is observed which is interpreted as a shell effect.We are able to determine the energy change Δ_{shell} which corresponds to the change in the level density using the Bethe level density expression[1]. The results presented as crosses in Fig. 16 have been calculated for even-odd nuclei. In order to cover the range of neutron number other elements have been included which are indicated with the element symbol. The results are included as crosses in Fig. 16 and the shell effect does not only reproduce the shift of 4.5 MeV but describes rather well the dependence upon the neutron number : the shift of the intruder states is due to a shell effect and characterises these states as intrinsic states. They behave differently to collective states in dependence of the neutron number.

In contrast to the assumption of Heyde et al.[1] there is no indication for a proton-neutron interaction.

A talk has been presented at the "Frühjahrstagung des Fachausschusses Kernphysik der DPG" in Groningen 1987 and another paper has been contributed to the 6th International Symposium on Capture Gamma-ray Spectroscopy in Leuven 1987.

---

(1) K.Heyde, P. Van Isacker, R.F. Casten, J.L. Wood, Phys. Letters 155 B (1985) 303 ; K. Heyde, J. Jolie, J. Moreau, J. Ryckebusch, M. Waroquier, P. Van Duppen, M. Huyse, J.L. Wood, Nucl. Phys. A466 (1987) 189

2 NUCLEAR METROLOGY

2.1 RADIONUCLIDE METROLOGY

International Comparison of Activity-Concentration Measurements of a ^{125}I Solution

D. Reher, E. Celen, C. Ballaux*

On behalf of Section II (Mesures des Radionucléides) of the CCEMRI the BIPM Sèvres, launched an international trial intercomparison of activity-concentration measurements of a ^{125}I solution. Seven laboratories, considered as leading in radionuclide metrology, were invited to participate in this comparison.

During the past years, the nuclide ^{125}I has been widely used in nuclear medicine. It decays by electron capture to an excited level of 35.5 keV in ^{125}I, which de-excites by a highly converted isomeric transition. Although ^{125}I has a simple decay scheme, it is rather difficult to standardize because of the low energies of the emitted radiations and the frequently present ^{126}I impurity. A large NaI(Tl) well-type detector was employed for the measurements of the low-energy photons. The so-called "sum-peak coincidence method" was used to obtain the decay rate of the sources from

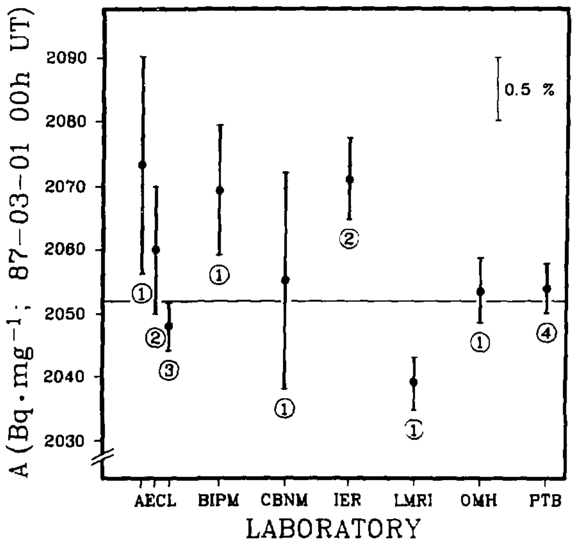

Fig. 17. Results of the ^{125}I trial comparison. The numbers refer to the four methods applied. 1) Sum-peak method, 2) X-X + (γ-γ) coincidences, 3) 4πe-X coincidence efficiency extrapolation, 4) photon-photon coincidence counting and efficiency-extrapolation method

* SCK/CEN, Mol, Belgium

the measured spectra. As can be seen from the results shown in Fig. 17, the value found at CBNM is in excellent agreement with those of the other participating laboratories.

Peak Analysis in High-Resolution Alpha-Particle Spectrometry

G. Bortels, P. Collaers*

A study to improve the accuracy of peak analysis in high-resolution alpha-particle spectrometry has been finished. Spectra were measured for which experimental conditions had been optimized in order to reduce peak distortion from various sources e.g. interfering impurity peaks and background, peak instability (mainly drift), peak summing (from alpha particles and coincident conversion electrons) and pile-up. These spectra were used to test the performance of a convolution-type peak-shape function.

The fitting model is based upon interpretation of the detection process in terms of simultaneous and mutually independent random processes which are each characterized by a probability-density function (PDF). These belong essentially to one of the following two types: a Gaussian PDF for processes such as electronic noise and straggling in very thin layers, or an asymmetric one for processes in which energy loss is the main effect, e.g. in scattering and by incomplete charge collection. For the latter an exponential PDF was proposed by L'Hoir(1). For independent processes the PDF for the overall process is the convolution of the individual PDFs.

Close examination of the peak asymmetry and tailing in our spectra indicated that an experimental alpha peak f(u) is well approximated by a convolution of the kind

$$f(u) = A\ G(u) * [(1-\eta)E_1(u) + \eta\ E_2(u) + C].$$

Here, G represents a normalized Gaussian, E_1 and E_2 are normalized exponentials, u is the energy variable, C is a constant which is obtained by normalizing to the height of the flat tail in the spectrum, η is a weighting factor and A is the number of counts in the peak. It can be shown that C can be eliminated from the model by performing a tail subtraction on the measured spectrum. This procedure does not require any information on the fine structure in the spectrum. The model then contains

---

* Presently at R. Bosch, Tienen, Belgium

(1) A. L'Hoir, Thèse 3ème cycle, Université Paris 7, unpublished (1975)

Table 4. Relative peak areas $A_i/\Sigma A_i$ and deduced activity and atom ratios from a fitted plutonium alpha-particle spectrum. Results are compared with emission probabilities P_α and data calculated from the NBS certificate of plutonium isotopic analysis. Uncertainties in units of the last decimal are indicated in brackets.

Nuclide	Energy E_α [keV]	$A_i/\Sigma A_i$	P_α *	Activity ratio	Atom ratio
^{241}Am	5442.9 5485.6	0.115(7) 0.866(20)	0.128(2) 0.852(8)	^{241}Am/^{238}Pu = 0.210(6) 0.228(2)*	^{238}Pu/^{239}Pu = $3.59(6)\cdot10^{-3}$ $3.48(4)\cdot10^{-3}$*
^{238}Pu	5456.5 5499.21	0.286(4) 0.713(6)	0.2884(6) 0.7104(4)		
^{239}Pu	5105.5 5143.8 5156.7	0.121(2) 0.167(5) 0.712(7)	0.118(2) 0.150(2) 0.731(7)	^{238}Pu/$^{239+240}$Pu = 0.519(9) 0.509(1)*	^{240}Pu/^{239}Pu = 0.245(5) 0.2410(1)*
^{240}Pu	5123.68 5168.17	0.272(4) 0.727(9)	0.270(5) 0.729(5)		

* Target Values

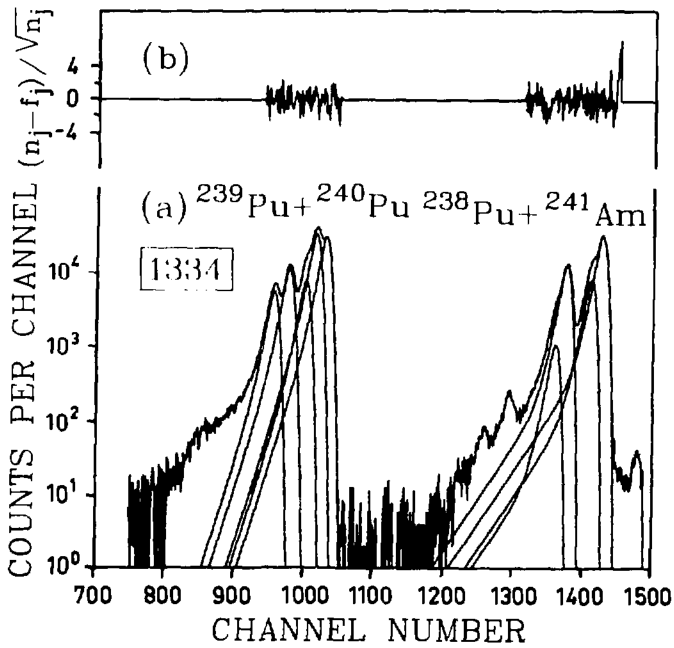

Fig. 18. a) Analysis of a plutonium spectrum. The ^{241}Am has grown into the source over a period of 2.643 years; b) weighted residuals from the fits

four shape parameters which are the same for all peaks in the spectrum and two specific parameters for each peak.

Figure 18 shows the results of the analysis of a plutonium spectrum from a sample of the NBS SRM 947 for a peak resolution of about 11.9 keV FWHM. The distribution of weighted residuals $(n_j-f_j)/\sqrt{n_j}$, where n_j is the number of counts in channel j and f_j is the function value at that channel, shows negligible structure. Results from the fit are given in Table 4. The deviation (2 %) of the plutonium activity ratio from the target value is due to the underestimated ^{241}Am ingrowth. A paper has been published.

Low-Energy X-Ray Standards

B. Denecke, G. Grosse and C. Ballaux*

A series of measurements was performed on Al-KX rays of 1.5 keV produced in an Al foil by fluorescence excitation with Mn-KX rays after electron capture of ^{55}Fe. Curve (a) in Fig. 19 displays a typical X-ray spectrum showing the Al-KX-ray peak situated on the low-energy tail of the Mn-KX-ray peak.

The ratio of the Mn-KX-ray and the Al-KX-ray emission rates is about 250. In the methane filled proportional counter only 5% of the 5.9 keV Mn-KX rays are detected and the rest is stopped in a lucite covered buffer chamber located on top of the counter (Fig. 20[1]). Some of the Mn-KX rays are backscattered from this volume into the counter and generate pulses to a significant low-energy tail which extends to the region of the Al-KX-ray peak. By increasing the length of the buffer chamber the tail contribution could be reduced by a factor of two. The tail was determined by covering the source with a 0.2 mm thick lucite foil to stop the Al-KX rays (Fig. 19 (b)).

The evaluation of the measured data is in progress. For the emission rates $N_t(\theta)$, measured within the cone half angle θ, various corrections have to be applied. Typical corrections for various window materials and gases

---

* SCK/CEN, Mol, Belgium

(1) C. Ballaux, First Interim Report, Contract CBNM/ST/87-87, 1988

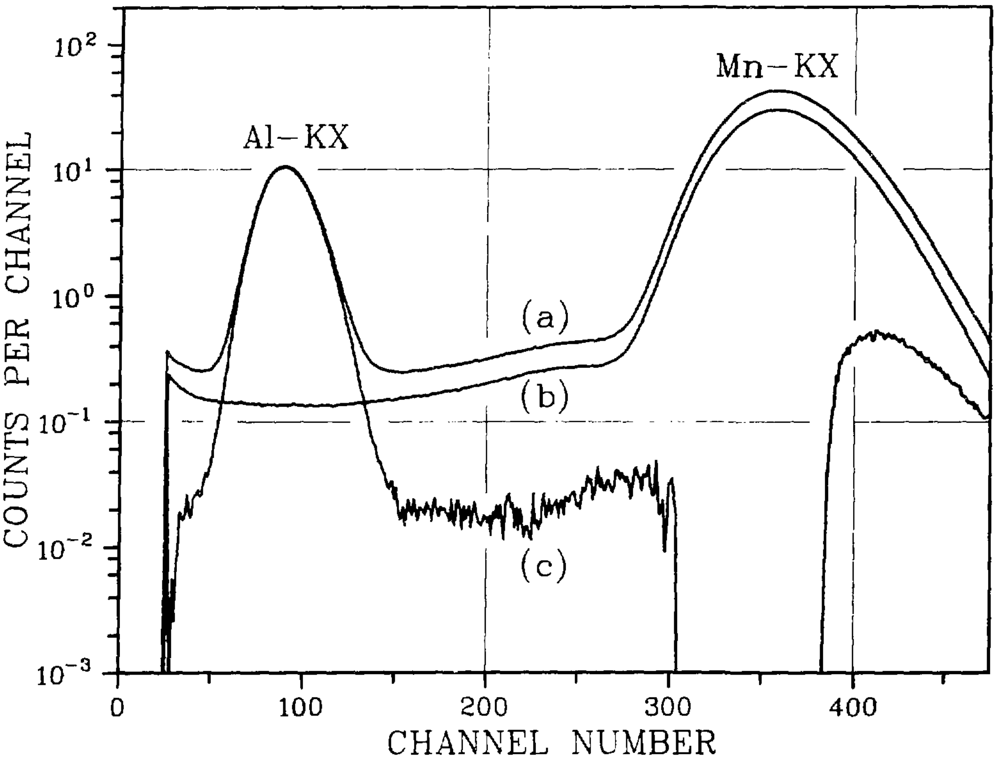

Fig. 19 X-ray spectra: (a) total spectrum, (b) spectrum with source covered by a 0.2 mm thick lucite foil to stop the Al KX rays, (c) net spectrum (a) - C xs (b), where C is a normalization factor.

were calculated[1] and listed in Table 5. It follows that hydrogen has a smaller absorption for the fluorescence KX rays and, in addition, a lower gas permeation rate through the counter window. Consequently, hydrogen is to be preferred to helium as source-chamber gas.

Problems which occured with the stability of the gas amplification of the proportional counter could be solved by using a modified electromagnetic valve at the outlet of the gas-flow system to control the gas density to within 0.1 %. To achieve this, it was necessary to insulate thermally both the counter and the pressure-reference vessel.

---

(1) W. Bambynek, CBNM Internal Report GE/R/RN/03/1986

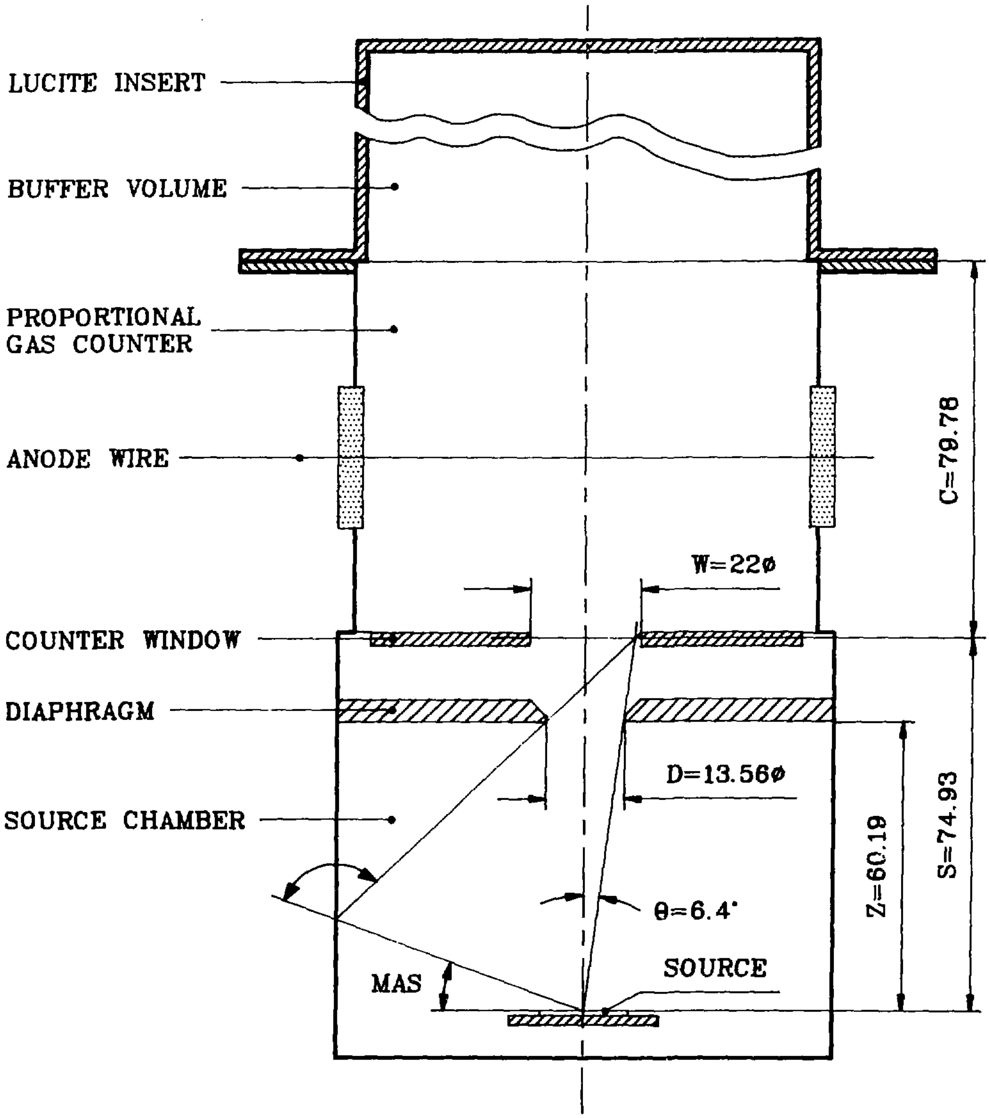

Fig. 20 Low-geometry X-ray counter. Dimensions (in mm) are given to calculate scattering and absorption effects. : θ cone half angle. Photons scattered at the chamber wall can only enter the proportional counter if the emission angle is smaller than MAS. The buffer volume and the proportional counter are separated by a 2 μm thick mylar foil coated with aluminium

Table 5. Typical corrections for the aluminium KX ray emission rate $N_t(\theta)$ when counting in a normalized solid angle $\Omega/4\pi$ = 3.142 10^{-3}

Correction due to	Factor
Source anisotropy	0.9986
Transmission T_G through the source chamber	
H_2: (ρ = 8.375 10^{-5} gcm^{-3})	0.999
He: (ρ = 1.847 10^{-4} gcm^{-3})	0.976
Transmission T_w through the detector window	
831 μgcm^{-2} hostaphane coated with 27 μgcm^{-2} Al	0.418
221 μgcm^{-2} mylar coated with 13 μgcm^{-2} Al	0.798
60 μgcm^{-2} formvar coated with 10 μgcm^{-2}	0.938
80 μgcm^{-2} polyimide coated with 27 μgcm^{-2} Al	0.918
200 μgcm^{-2} polyimide coated with 27 μgcm^{-2} Al	0.822
Efficiency of the counter filled with CH_4	0.960

Measurement conditions: 22 °C, 0.113 MPa.

Length of source chamber: 75 mm, length of counter: 80 mm.

Uncertainty Assignment

W. Bambynek

An invited lecture "Uncertainty Assigment in Radionuclide Metrology" was given at the First International Summer School on Low-Level Measurements and their Aprlications to Environmental Radioactivity, La Rábida, Spain. The various problems how to assign properly uncertainties to the results of measurements were discussed. The basic principles were outlined and methods were indicated for the estimation of variances and covariances. The general expression for the propagation of uncertainties was derived. Examples were taken from the field of radionuclide metrology.

2.2 METROLOGY OF NEUTRON FLUX AND DOSE

Neutron Calorimetry

A.Paulsen*, R. Widera, H. Nerb

A report[1] has been written, summarizing the experience during construction, operation and calibration of the CBNM tissue equivalent plastic (TEP) absorbed dose calorimeter. The low thermal diffusivity of TEP causes considerable difficulties compared to the case of graphite. A new TEP calorimeter would need to have more uniform electrical heating of the calorimeter bodies, compared to the pointwise heating realized in the present versions. The sensitivity of the TEP calorimeter is only 21 Gy/V, compared to 8.8 Gy/V for the graphite calorimeter , which is mainly due to the difference in specific heat capacity of graphite and TEP. Due to lack of manpower this line of research has been discontinued.

International Fluence Comparison

H. Liskien, R. Widera

To check the usefulness of the two spheres technique, BIPM has organized a mini-intercomparison on neutron fluence determination involving NPL Teddington, NBS Washington, PTB Braunschweig, CBNM Geel and BIPM Sèvres. Tests are to be carried out at two energies (2.5 and 14.65 MeV) employing a spherical ^{3}He proportional counter (SP 90) and two moderating spheres (8.9 and 21.4 cm diameter) Measurements with two different spheres and at various source-detector distances should allow calculational discrimination of these disturbing neutrons. The detectors have been received from PTB Braunschweig and preparatory work has been performed for the final measurements to be carried out in early 1988.

Neutron Ionometry.

H. Liskien, R. Widera

Absorbed-dose determinations by ionometric techniques were performed in connection with neutron irradiations for the Radiobiology Department of SCK/CEN Mol. To study late effects in the brain of adult rats which had suffered low dose irradiations during their embryonic life, already in

---

* retired

(1) A. Paulsen, R. Widera, H. Nerb, CBNM Internal Report GE/R/VG/54/1987

1985 animals have been irradiated in utero with 0.6 and 2.5 MeV neutrons and doses of 2.5, 5, 10 and 15 cGy. It seemed from this experiment that an effect is still significant down to doses of 2.5 cGy. Therefore this experiment was continued in 1987 by irradiating further 17 pregnant rats with 0.6 MeV neutrons and doses of 1 and 2.5 cGy.

TECHNICAL APPENDIX

Van de Graaff Accelerators

A. Crametz, P. Falque, J. Leonard, W. Schubert

KN - 3.7 MV : the beam tube extension at 15° left after the switching magnet is fully equipped for Rutherford backscattering measurements and the equipment at the 30° right beam tube is under installation for PIXE experiments. The photograph (Fig. 21) shows the new target hall. Because this target hall is situated near the entrance of the building, an adequate security system has been realized to allow only authorized persons to enter the hall and to interrupt the beam with a shutter valve whenever safety conditions are not fulfilled.

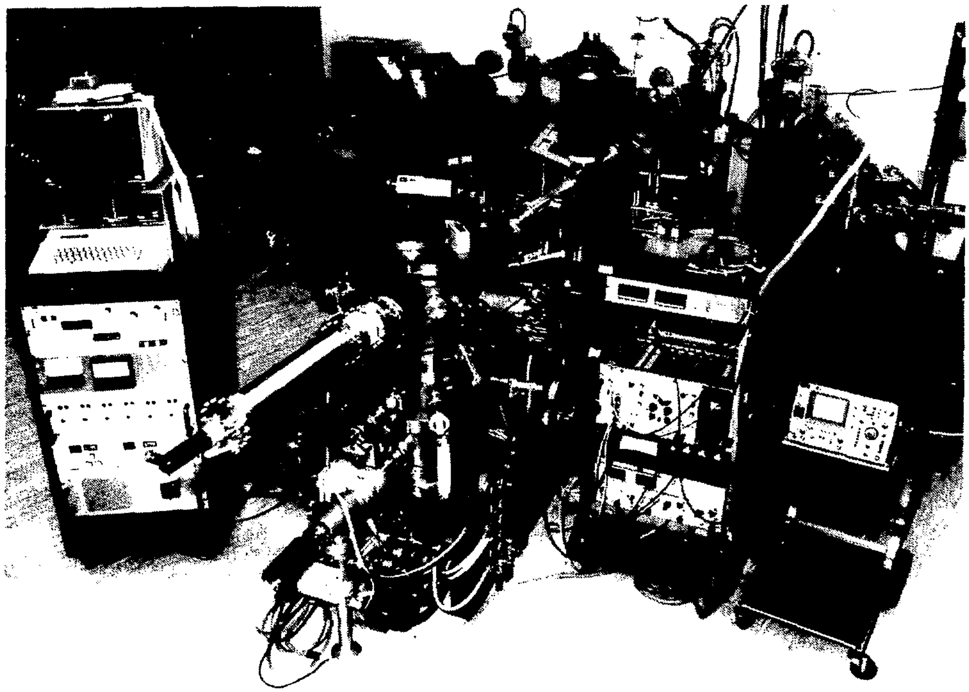

Fig. 21. New target hall with RBS experimental set-up

CN - 7 MV: for neutron dosimetry work, the use of a strong neutron source via the ^{9}Be(d,n) reaction as well as a strong γ-ray source from a 250Ci ^{137}Cs source at level 0 m, necessitated a complete renewal of the security system as represented by the flow-chart shown in Fig. 22. In reality, the radiation field is a mixed neutron/γ-ray field and the γ-ray component has to be determined by using a pure γ-ray field.

The first 20 meters of the 40 m long flight path have been installed inside the building. The 20 m outside will be mounted when first results are available.

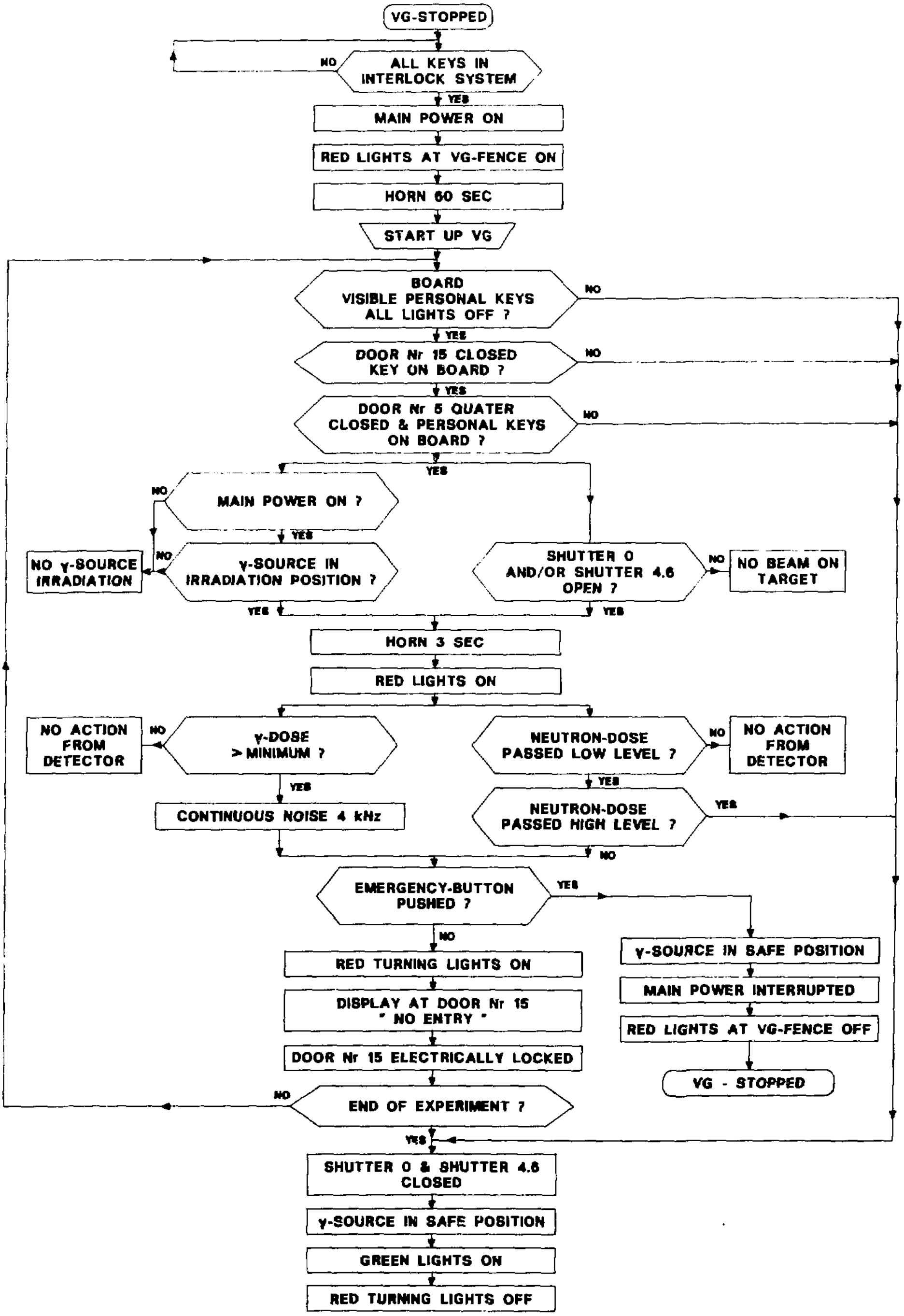

Fig. 22. CN-7 MV : shutter control and irradiation protection scheme

LIST OF PUBLICATIONS

CONTRIBUTION TO CONFERENCES

BABELIOWSKY, T., HORSTMANN, H., CERVINI, C.
High-speed communication between Ethernet and MVS.
SEAS Anniversary Meeting, Edinburgh, September 28 - October 2, 1987

BAMBYNEK, W.
Radionuclide data.
Proc. Intern. Summer School on Low-Level Measurements and their Applications to Environmental Radioactivity, La Rábida, September 27 - October 10, 1987; M. Garcia-Leon and G. Madurga (eds.), World Sci. Publ. Co., Singapore (1988), p. 3

BAMBYNEK, W.
Radionuclide data.
Uncertainty assignment in radionuclide metrology.
Ibidem, p. 23

BÖCKHOFF, K.H.
Electron linac based pulsed white neutron sources for high resolution neutron time of flight spectroscopy. - Status and perspectives.
Proc. IAEA Advisory Group Meeting on Properties of Neutron Sources, IAEA, Vienna (1987), p. 35

BÖCKHOFF, K.H.
Electron linacs and beyond.
Ibidem, p. 408

CORVI, F.
Experimental determination of the weighting function of a total energy γ-ray detector.
Intern. Conf. on Neutron Physics, Kiev, September 21 - 25, 1987

CORVI, F., PREVIGNANO, A., SMITH, P., GASPERINI, F.
Experimental determination of the response function of a γ-ray detector in the range 0.5 - 10 MeV.
6^{th} Intern. Symp. on Capture Gamma-Ray Spectroscopy, Leuven, August 31 - September 4, 1987

DERUYTTER, A.J., WAGEMANS, C., CORVI, F., AXTON, E.J., SCHILLEBEECKX, P.
Recent differential low energy cross-sections and thermal evaluations.
IAEA AGM on Meas. Nucl. Data for the Calcul. of Thermal Reactivity Coeff., Vienna, December 7-11, 1987

FETTWEIS, P., QUIK, F.
Some considerations on Pu gamma branching ratios resulting from calibration runs performed with the help of PuO_2-reference samples of well defined isotopic composition.
9th Annual ESARDA Symp. on safeguards and Nuclear Materials Management, London, May 12-14, 1987

HAMBSCH, F.-J., KNITTER, H.-H., BUDTZ-JØRGENSEN, C., MUTTERER, H., THEOBALD, J.P.
Early and late stages of low energy nuclear fission fragment mass-, energy- and shape-fluctuations.
Intern. Conf. on Collective Phenomena in Nuclear and Subnuclear Long-Range Interactions in Nuclei, Bad Honnef, May 4 - 7, 1987

HAMBSCH, F.-J., KNITTER, H.-H., BUDTZ-JØRGENSEN, C., STRAEDE, CH., THEOBALD, J.P.
Fission modes in $^{235}U(n,f)$.
Intern. Conf. on Neutron Physics, Kiev, September 21 - 25, 1987

HAMBSCH, F.-J.,KNITTER, H.-H., BUDTZ-JØRGENSEN, C., THEOBALD, J.P.
Neutron induced fission of ^{235}U below 0.5 MeV.
Frühjahrstagung des Fachauschusses Kernphysik der DPG, Groningen, March 23 - 27, 1987; Verhandlungen DPG 4 (1987) PC-37

ROHR, G.H.
Intruder states: result of different energy behaviour of intrinsic and collective states.
6^{th} Intern. Symp. on Capture Gamma-Ray Spectroscopy Leuven, August 31 - September 4, 1987

ROHR, G.H.
Doorway structures in $^{28}Si+n$ and $^{32}S+n$ based on discontinuities of the level spacing.
Ibidem

ROHR, G.
A simple explanation for intruder states studied with Cd and Pb isotopes.
Frühjahrstagung des Fachausschusses Kernphysik der DPG, Groningen.
March 23 - 27, 1987; Verhandlungen DPG 4 (1987) G2, 6

WAGEMANS, C., SCHILLEBEECKX, P., DERUYTTER, A., BARTHELEMY, R.
Mass and energy distributions for the spontaneously fissioning plutonium isotopes.
Frühjahrstagung des Fachausschusses Kernphysik der DPG, Groningen,
March 23 - 27, 1987; Verhandlungen DPG 4 (1987) C2, 1

WAGEMANS, C., SCHILLEBEECKX, P., DERUYTTER, A., BARTHELEMY, R.
Fission physics experiments at the BR1 reactor.
Intern. Symp. on Utilization of Multipurpose Research Reactors and Related International Cooperation, Grenoble, October 19 - 23, 1987

WAGEMANS, C., WEIGMANN, H., BARTHELEMY, R.
Nuclear structure studies with (n,α) and (n,p) reactions.
6th Intern. Symp. on Capture Gamma-Ray Spectroscopy, Leuven, August 31 - September 4, 1987

WARTENA, J.A., WEIGMANN, H., BÜRKHOLZ, C.
Preliminary results of η of ^{235}U for subthermal neutron energies.
IAEA AGM on meas. Nucl. Data for the Calcul. of Thermal Reactivity Coeff., Vienna, December 7-11, 1987

WEIGMANN, H.
Neutron Spectroscopy with GELINA.
Proc. Vth Intern. School on Neutron Physics, Alushta (1986), p. 47

WEIGMANN, H.
Summary on nuclear structure at high excitations and nuclear reactions.
6th Intern. Symp. on Capture Gamma-Ray Spectroscopy, Leuven, August 31 - September 4, 1987

WEIGMANN, H., KÖHLER, R., POORTMANS, F., RAMAN, S., WARTENA, J.A.
Ground state partial radiative widths of ^{207}Pb+n resonances and M1 and E2 strengths in ^{208}Pb.
Ibidem

WEIGMANN, H., MARTIN, P., POORTMANS, F., WARTENA, J.A.
Ground state partial radiative widths of ^{28}Si+n resonances.
Ibidem

SCIENTIFIC OR TECHNICAL ARTICLES

BORTELS, G., COLLAERS, P.
Analytical function for fitting peaks in alpha-particle spectra from Si detectors.
Appl. Radiat. Isot., Int. J. Radiat. Appl. Instrum. Part A 38 (1987) 831

BUTDZ-JØRGENSEN, C., KNITTER, H.-H., STRAEDE, CH., HAMBSCH, F.-J., VOGT, R.
A twin ionization chamber for fission fragment detection.
Nucl. Instr. Methods Phys. Res. A258 (1987) 209

CORVI, F., PREVIGNANO, A., LISKIEN, H., SMITH, B.P.
An experimental method for determining the total efficiency and the response function of a gamma-ray detector in the range 0.5 - 10 Mev.
Nucl. Instr. Methods Phys. Res. A265 (1988) 475

D'EER, A., WAGEMANS, C., NEVE DE MEVERGNIES, M., GÖNNEWEIN, F., GELTENBORT, P., MOORE, M.S., PAUWELS, J.
Neutron induced fission of the 26 min uranium-235 isomer.
Phys. Rev. C (to be published)
DEKEMPENEER, E., LISKIEN, H., MEWISSEN, L., POORTMANS, F.
A spectrometer for double-differential neutron-emission cross section measurements in the energy range 1.6 to 16 MeV.
Nucl. Instr. Methods Phys. Res. A256 (1987) 489

DEKEMPENEER, E., LISKIEN, H., MEWISSEN, L., POORTMANS, F.
Double-differential neutron-emission cross sections for ^{7}Li and incident neutrons between 1.6 and 13.8 MeV.
Nucl. Sci. Eng. 97 (1987) 353

DENECKE, B.
Measurements of the 59.5 keV gamma-ray emission probability in the decay of ^{241}Am with a 4π-CsI(Tl)-sandwich spectrometer.
Appl. Radiat. Isot., Int. J. Radiat. Appl. Instrum. Part A 38 (1987) 823

HAMBSCH, F.-J.
Untersuchungen der Massen- und Energieverteilung der neutroneninduzierten Spaltung von ^{235}U im Bereich aufgelöster Resonanzen.
Dissertation, D-17, Darmstadt (1987)

KNITTER, H.-H., BUDTZ-JØRGENSEN, C.
Neutron induced fission cross section of ^{243}Am in the energy range from 1 MeV to 10 MeV.
Nucl. Sci. Eng. 99 (1988)1

KNITTER, H.-H., HAMBSCH, F.-J., BUDTZ-JØRGENSEN, C., THEOBALD, J.P.
Three exit channels in the fission of ^{235}U(n,f).
Z. Naturforsch. 42a (1987) 786

KÖHLER, R., WARTENA, J.A., WEIGMANN, H., MEWISSEN, L., POORTMANS, F., THEOBALD, J.P., RAMAN, S.
Nuclear structure of ^{208}Pb from ^{207}Pb+n resonances.
Phys. Rev. C35 (1987) 1646

LISKIEN, H., WIDERA, R., WÖLFLE, R., QAIM, S.M.
Experimentally determined excitation function for the ^{9}Be(n,t) reaction.
Nucl. Sci. Eng. 98 (1988) 266

PAUWELS, J., EYKENS, R., D'EER, D., WAGEMANS, C., NEVE DE MEVERGNIES, M.
The preparation of a ^{239}Pu mother source for the production of ^{235}U targets.
Nucl. Instr. Methods Phys. Res. A257 (1987) 21

SCHMIEDER, L., HILSCHER, D., ROSSNER, R., JAHNKE, U., LEHMANN, M., ZIEGLER, K., KNITTER, H.-H.
Neutron yields of ^{6,7}Li-induced reactions on thick ^{7}Li, ^{9}Be, ^{12}C and ^{nat}Cu-targets.
Nucl. Instr. Methods Phys. Res. A256 (1987) 457

STRAEDE, CH., BUDTZ-JØRGENSEN, C., KNITTER, H.-H.
^{235}U(n,f) fragment mass-, kinetic energy- and angular distributions for incident neutron energies between thermal and 6 MeV.
Nucl. Phys. A462 (1987) 85

WAGEMANS, C., WEIGMANN, H., BARTHELEMY, R.
Measurements and resonance analysis of the $^{33}S(n,\alpha)$ cross section.
Nucl. Phys. A469 (1987) 497

WEIGMANN, H., MARTIN, P.W., KÖHLER, R., VAN PARIJS, I., POORTMANS, F., WARTENA, J.A.
Structure of unbound states in ^{29}Si from neutron resonance spectroscopy of ^{28}Si+n.
Phys. Rev. C36 (1987) 585

WÖLFLE, R., MANNAN, A., QAIM, S.M., LISKIEN, H., WIDERA, R.
Excitation functions of $^{93}Nb(n,2n)^{92m}Nb$, $^{93}Nb(n,\alpha)^{90m,g}Y$, $^{139}La(n,\alpha)^{136}Cs$ and $^{181}Ta(n,p)^{181}Hf$ reactions in the energy range of 12.5 to 19.6 MeV.
Appl. Radiat. Isot., Int. J. Radiat. Appl. Instrum. Part A 39 (1988) 407

SPECIAL PUBLICATIONS

HANSEN, H.H. (ed.)
Annual Progress Report on Nuclear Data 1986.
NEANDC (E) 282 "U", Vol. III Euratom; INDC (EUR) 021/G (1987)

GLOSSARY

A E C L	Atomic Energy of Canada Limited, Chalk River (Canada)
A E R E	Atomic Energy Research Establishment, Harwell (GB)
A G M	Advisory Group Meeting
A N S	American Nuclear Society
B I P M	Bureau International des Poids et Mesures, Sèvres (F)
C B N M	Central Bureau for Nuclear Measurements (JRC-Geel), Geel (B)
C C E M R I	Comité Consultatif pour les Etalons de Mesure des Rayonnements Ionisants
C E A	Commissariat à L'Energie Atomique, Paris (F)
C E C	Commission of the European Communities
C I E M A T	Centro de Investigaciones Energetica Medio Ambiental y Tecnologicas, Madrid (E)
C M	Centre of mass
C R P	Coordinated Research Programme
D P G	Deutsche Physikalische Gesellschaft
E C	European Community
E N D F	Evaluated Nuclear Data File
E P F L	Ecole Polytechnique Fédérale de Lausanne, Lausanne (CH)
E S A R D A	European Safeguards Research and Development Association
E T L	Electrotechnical Laboratory, Ibaraki (Japan)
G D	General Direction
G E L I N A	Geel Electron Linear Accelerator
I A E A	International Atomic Energy Agency, Vienna (A)
I E R	Institut d'Electrochimie et Radiochimie de l'EPFL, Lausanne (CH)
I C R M	International Committee for Radionuclide Metrology
I L L	Institut Laue-Langevin, Grenoble (F)
I N D C	International Nuclear Data Committee
I R K	Institut für Radiumforschung und Kernphysik, Wien (A)
J E F	Joint European File
J E N D L	Japanese Evaluated Data Library
J R C	Joint Research Centre
K F A	Kernforschungsanlage, Jülich (D)
L M R I	Laboratoire de Métrologie des Rayonnements Ionisants, Saclay (F)
N B S	National Bureau of Standards, Gaithersburg (U S A)
N E A	Nuclear Energy Agency, Paris (F)

N E A C R P	Nuclear Energy Agency's Committee for Reactor Physics
N E A N D C	Nuclear Energy Agency's Nuclear Data Committee
N I M	National Institute of Metrology, Beijing (PR of China)
N P L	National Physical Laboratory, Teddington (GB)
N R C	National Research Council of Canada, Ottawa (Canada)
O E C D	Organization for Economic Cooperation and Development
O M H	Orzágos Mérésügyi Hivatal, Budapest (H)
O R N L	Oak Ridge National Laboratory, Oak Ridge (USA)
P P R	Programme Progress Report
P T B	Physikalisch-Technische Bundesanstalt, Braunschweig (FRG)
S C K/ C E N	Studiecentrum voor Kernenergie/ Centre d'Etudes Nucléaires, Mol (B)
S R M	Standard Reference Material
W R E N D A	World Request List for Neutron Data Measurements

CINDA ENTRIES LIST

ELEMENT		QUANTITY	TYPE	ENERGY		DOCUMENTATION		LAB	COMMENTS
S	A			MIN	MAX	REF VOL PAGE	DATE		
U	235	FRS	EXPTL-PROG	30-2	50+5	INDC(EUR)22G0001	-88	GEL	KNITTER + LINAC MASS ANG DIST
CF	252	SFN	EXPTL-PROG			INDC(EUR)22G0006	-88	GEL	BUDTZ + FISS PROD MASS ANG DIST
U	233	NF	EXPTL-PROG	10-3	10+1	INDC(EUR)22G0014	-88	GEL	WAGEMANS + LINAC SIMULT ANALYSIS
U	235	NF	EXPTL-PROG	10-3	10+1	INDC(EUR)22G0014	-88	GEL	WAGEMANS + LINAC SIMULT. ANALYSIS
PU	239	NF	EXPTL-PROG	10-3	10+1	INDC(EUR)22G0014	-88	GEL	WAGEMANS + LINAC SIMULT ANALYSIS
U	235	ETA	EXPTL-PROG	20-3	30-1	INDC(EUR)22G0015	-88	GEL	WEIGMANN + LINAC CORRECTIONS
U	235	NF	EXPTL-PROG	10-7	10-4	INDC(EUR)22G0017	-88	GEL	WAGEMANS + ILL COLD SOURCE CHOPPER
PU	236	SFN	EXPTL-PROG			INDC(EUR)22G0018	-88	GEL	DERUYTTER + MASS ENERGY DIST
CR	052	N2N	EXPTL-PROG	TR	20+7	INDC(EUR)22G0018	-88	GEL	LISKIEN + VDG EXCITATION FUNCTION
MO	092	NP	EXPTL-PROG	13+7	20+7	INDC(EUR)22G0019	-88	GEL	LISKIEN + VDG EXCITATION FUNCTION
MO	095	NF	EXPTL-PROG	13+7	20+7	INDC(EUR)22G0019	-88	GEL	LISKIEN + VDG EXCITATION FUNCTION
MO	096	NP	EXPTL-PROG	13+7	20+7	INDC(EUR)22G0019	-88	GEL	LISKIEN + VDG EXCITATION FUNCTION
MO	092	NA	EXPTL-PROG	13+7	20+7	INDC(EUR)22G0019	-88	GEL	LISKIEN + VDG EXCITATION FUNCTION
MO	098	NA	EXPTL-PROG	13+7	20+7	INDC(EUR)22G0019	-88	GEL	LISKIEN + VDG EXCITATION FUNCTION
MO	100	NA	EXPTL-PROG	13+7	20+7	INDC(EUR)22G0019	-88	GEL	LISKIEN + VDG EXCITATION FUNCTION
NB	093	N2N	EXPTL-PROG	13+7	20+7	INDC(EUR)22G0019	-88	GEL	LISKIEN + VDG EXCITATION FUNCTION
NB	093	NA	EXPTL-PROG	13+7	20+7	INDC(EUR)22G0019	-88	GEL	LISKIEN + VDG EXCITATION FUNCTION
LA	133	NA	EXPTL-PROG	13+7	20+7	INDC(EUR)22G0019	-88	GEL	LISKIEN + VDG EXCITATION FUNCTION
TA	181	NP	EXPTL-PROG	13+7	20+7	INDC(EUR)22G0019	-88	GEL	LISKIEN + VDG EXCITATION FUNCTION
FE	056	TOT	EXPTL-PROG	11+3	11+3	INDC(EUR)22G0020	-88	GEL	CORVI + WEIGHTING C6D6 DETECTOR
NB	093	SIN	EXPTL-PROG	79+6	79+6	INDC(EUR)22G0023	-88	GEL	LISKIEN + ACTIVATION
LI	007	NXN	EXPTL-PROG	16+6	14+7	INDC(EUR)22G0025	-88	GEL	LISKIEN + DOUBLE DIFF EMISSION
BE	009	NT	EXPTL-PROG	13+7	20+7	INDC(EUR)22G0026	-88	GEL	LISKIEN + EXCITATION FUNCTION
BE	009	NT	EXPTL-PROG	15+6	90+6	INDC(EUR)22G0026	-88	GEL	WEIGMANN + DOUBLE DIFF EMISSION
NI	060	NA	EXPTL-PROG	50+6	14+6	INDC(EUR)22G0028	-88	GEL	WATTECAMPS RATIO TO NIo58(NA)
CU	063	NA	EXPTL-PROG	50+6	14+6	INDC(EUR)22G0028	-88	GEL	WATTECAMPS RATIO TO NIo58(NA)
CU	065	NA	EXPTL-PROG	50+6	14+6	INDC(EUR)22G0028	-88	GEL	WATTECAMPS RATIO TO NIo58(NA)
SI	028	RES	EXPTL-PROG	30+4	30+6	INDC(EUR)22G0030	-88	GEL	WEIGMANN M1 AND E2 STRENGTH
SI	028	RES	EXPTL-PROG	10+5	30+6	INDC(EUR)22G0030	-88	GEL	ROHR + DOORWAY STRUCTURE
S	032	RES	EXPTL-PROG	10+5	20+6	INDC(EUR)22G0030	-88	GEL	ROHR + DOORWAY STRUCTURE
CA	041	NA	EXPTL-PROG	50+3	10+6	INDC(EUR)22G0033	-88	GEL	WAGEMANS + ION CHAMBER
PB	207	RES	EXPTL-PROG	50+3	10+6	INDC(EUR)22G0033	-88	GEL	WEIGMANN
PB	208	RES	EXPTL-PROG	70+6	90+6	INDC(EUR)22G0033	-88	GEL	WEIGMANN M1 AND E2 STRENGTH